Chapter 3
Production of Dioxygen in the Dark: Dismutases of Oxyanions

Jennifer L. DuBois and Sunil Ojha

Contents

J.L. DuBois (✉) • S. Ojha
Department of Chemistry and Biochemistry, Montana State University, Bozeman, MT 59717, USA
e-mail: jdubois@chemistry.montana.edu

P.M.H. Kroneck, M.E. Sosa Torres (eds.), *Sustaining Life on Planet Earth: Metalloenzymes Mastering Dioxygen and Other Chewy Gases*, Metal Ions in Life Sciences 15, DOI 10.1007/978-3-319-12415-5_3

Abstract O_2-generating reactions are exceedingly rare in biology and difficult to mimic synthetically. Perchlorate-respiring bacteria enzymatically detoxify chlorite (ClO_2^-), the end product of the perchlorate (ClO_4^-) respiratory pathway, by rapidly converting it to dioxygen (O_2) and chloride (Cl^-). This reaction is catalyzed by a heme-containing protein, called chlorite dismutase (Cld), which bears no structural or sequence relationships with known peroxidases or other heme proteins and is part of a large family of proteins with more than one biochemical function. The original assumptions from the 1990s that perchlorate is not a natural product and that perchlorate respiration might be confined to a taxonomically narrow group of species have been called into question, as have the roles of perchlorate respiration and Cld-mediated reactions in the global biogeochemical cycle of chlorine. In this chapter, the chemistry and biochemistry of Cld-mediated O_2 generation, as well as the biological and geochemical context of this extraordinary reaction, are described.

Keywords chlorite • dioxygen • heme • perchlorate • peroxidases

Please cite as: *Met. Ions Life Sci.* 15 (2015) 45–87

1 Introduction

The S4 state of photosystem II (PSII) – the catalytic species poised to make the O=O bond of O_2 – is one of the most sought-after, and most elusive, chemical structures in the history of biological chemistry [1, 2]. In spite of years of effort and a wide spectrum of approaches, the particulars of how PSII makes this deceptively simple bond are still controversial. At the same time, nature offers few other paradigms for reactions that couple two oxygen atoms. Currently, there is just one other known natural process: chlorite (ClO_2^-) is converted to chloride (Cl^-) and dioxygen (O_2) by an enzyme called chlorite dismutase (Cld).

These two systems make for an interesting comparison. PSII is an exceedingly complicated, membrane-associated molecular machine, comprised of around 20 protein subunits (depending on the organism) and a series of cofactors including 35 chlorophyll a molecules, 12 β-carotenes, two pheophytins, two plastoquinones,

two hemes, one bicarbonate, 20 accessory lipids, and one non-heme Fe^{2+}, all in addition to the famous distorted cubane Mn_4CaO_5 cluster where O_2 evolution takes place [3]. This impressive apparatus harvests energy from light, using it to drive an exquisitely timed series of electron and proton transfers that result in the net splitting of water and emission of O_2 gas.

In sharp contrast to PSII, Cld is a relatively simple, water-soluble heme enzyme that, outside of making an O=O bond with exquisite efficiency, has little else to do [4]. As a consequence, Cld provides a window into one set of electronic and structural requirements for joining a pair of O atoms under biological conditions. Understanding the Cld reaction may therefore yield some analogies for PSII-S4 and perhaps synthetic, structurally still simpler water-splitting catalysts. At the same time, the Cld reaction extends the known repertoire of heme catalysis since, though many heme proteins and model complexes react with chlorite, the issuance of O_2 from any of them is an exceedingly rare outcome. The following chapter describes the structures and chemical mechanisms of the Clds, their diversity, and what is currently known about the geochemical and biological forces that gave rise to this type of catalysis. It concludes with a summary of some of the relevant small molecule and heme protein chemical reactivity with chlorite, asking effectively why they are *not* "Clds," and what limits O_2 generation in these cases.

2 Geochemistry of the Oxochlorates

Any thermodynamically well-matched combination of electron source and sink, no matter how exotic, can seemingly be found driving the metabolism of some microbial species. The oxyanions of main group elements such as nitrogen, sulfur, selenium, and arsenic, organic compounds of nitrogen and sulfur, and even solid mineral species (manganese, iron) can all serve as respiratory electron acceptors, provided that an electron donor with a larger reduction potential is available in the same environment. The redox tower diagram illustrates this point, listing several "edibles" (electron sources) and "breathables" (electron sinks) known to be used by various microbial species (Figure 1) [5]. Metabolism of these elements benefits the microbe, and at the same time strongly impacts global geochemical element cycles.

The ability to assume or toggle between different metabolic strategies depends on the presence of the appropriate enzymatic pathways in the microbe's genome. Some environmental microbes appear to be avid collectors of such pathways, duplicating and transferring them laterally from species to species and providing the raw materials from which new metabolic capabilities can emerge. Evolution, however, depends on the presence of environmental selection pressures to drive it. Microbial perchlorate respiration therefore was a surprise when it was first discovered in the late 1990s [6–11]. At that time, perchlorate was assumed to be almost exclusively a man-made chemical species with few known natural repositories. Wide-scale industrial production of perchlorate as a rocket propellant,

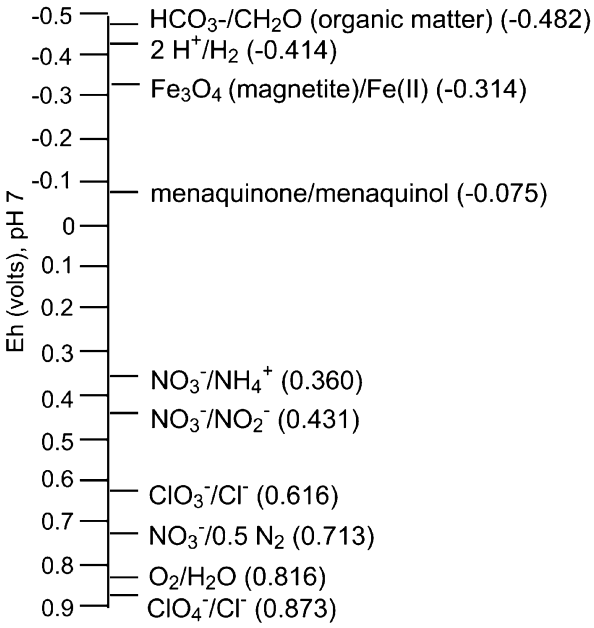

Figure 1 Redox tower, showing potential electron donors and acceptors used by microbes. The electron donor ("edible") and acceptor ("breathable") must together yield a process that is thermodynamically downhill. In terms of the tower, the edible must be higher than the chosen breathable. Tower data are adapted from reference [5].

constituent of fireworks and explosives, and chemical oxidant moreover only began in the U.S. in 1910 [12], and was increasingly identified as a freshwater pollutant at around the same time that perchlorate-respiring bacteria were discovered [13, 14]. The evolution of microbial perchlorate respiration therefore would have had to occur very quickly in response to man-made perchlorate, or in response to natural sources of perchlorate that had yet to be discovered. Which could it be?

Among other evidence, the identification of perchlorate respiration in diverse microbes from geographically far-flung locales, including places untainted by man-made oxochlorates, now suggests that perchlorate and bacteria that can eliminate it have indeed been with us for a long time. Perchlorate respiration in fact appears to play a pivotal and previously unappreciated role in the global cycling of chlorine. It is also potentially responsible for the dramatically different distribution of perchlorate on the surface of the Earth *versus* Mars, as described below.

2.1 Oxochlorates as Respiratory Anions

Using perchlorate as a terminal electron sink in respiratory pathways makes great chemical sense. It is highly water-soluble [14], a fact that also colors its ability to distribute in soils and travel in groundwaters [15]. Thermodynamically, it is a powerful electron acceptor. The standard reduction potential for the complete reduction of perchlorate to chloride is on par with the five-electron reduction of

nitrate (a more biologically common respiratory anion), or the four-electron reduction of O_2 [14, 16, 17]:

$$ClO_4^- + 8\ H^+ + 8\ e^- \rightarrow Cl^- + 4\ H_2O \quad E^\circ = 1.287\ V \quad (1)$$

$$NO_3^- + 6\ H^+ + 5\ e^- \rightarrow \tfrac{1}{2}\ N_2 + 3\ H_2O \quad E^\circ = 0.713\ V \quad (2)$$

$$O_2 + 4\ H^+ + 4\ e^- \rightarrow 2\ H_2O \quad E^\circ = 1.229\ V \quad (3)$$

The successive reductions of chlorate (Cl^{5+}) to chlorite (Cl^{3+}), chlorite to hypochlorite (Cl^{1+}), and hypochlorite to Cl^- are likewise highly thermodynamically favored [14, 18, 19]:

$$ClO_3^- + 2\ H^+ + 2\ e^- \rightarrow ClO_2^- + H_2O \quad E^\circ = 1.201\ V \quad (4)$$

$$ClO_2^- + 2\ H^+ + 2\ e^- \rightarrow ClO^- + H_2O \quad E^\circ = 1.645\ V \quad (5)$$

$$ClO^- + 2\ H^+ + 2\ e^- \rightarrow Cl^- + H_2O \quad E^\circ = 1.49\ V \quad (6)$$

Biologically, reduction of perchlorate to the product chlorate or chlorate to chlorite occurs with transfer of an oxygen atom, which in each case is protonated to form water. Facilitating proton transfer is consequently likely to be important for each of these reductions. Note that all of the reactants and products are written here as anions, though the standard potentials are reported (pH = 0, *versus* NHE) and the pK_as of their proton dissociation reactions ($HClO_x \rightleftharpoons ClO_x^- + H^+$) span a very broad range: −10 (ClO_4^-), −1 (ClO_3^-), 1.72 (ClO_2^-), 7.5 (ClO^-), and −8 (Cl^-) [14, 19, 20].

Finally, perchlorate is also a good bet from a kinetic perspective. Like O_2, its reactions with many potential reductants tend to be slow [14]. As a consequence, perchlorate is relatively stable under aqueous/biological conditions. Rather than simply "burning up" in a biological matrix, its thermodynamically favored reduction, like O_2's, would need to be catalyzed.

2.2 *Natural Abundance of Perchlorate on Earth*

From a geological perspective, perchlorate seems a decidedly unattractive electron acceptor because it has not accrued to nearly the same extent as O_2 or nitrate, either on land or at sea [21]. Naturally occurring perchlorate at its most abundant can be found comingled with deposits of sodium nitrate in the Atacama Desert of northern Chile (see Figure 2 in Section 2.4). These deposits have been heavily mined as sources for nitrate-based fertilizers. Chilean nitrate is in fact estimated to be the source of ~81×10^6 kg of perchlorate imported to the U.S. (1909–1997) [22–24]. The Atacama itself is a highly unusual, arid, and geologically exotic place. It is believed to have persisted as a nearly rainless climate for 10–15 million years, over which time its nitrate deposits have accumulated. The arid climate and general lack of hydrologic events or large scale biotic (including human) incursions may be responsible for the preservation of the nitrate deposits and for the

co-concentration of ions like perchlorate and chromate, which are otherwise not found in large amounts anywhere on earth [25]. These deposits have been shown to have a distinct oxygen isotope pattern, making it possible to distinguish natural and synthetic perchlorate [26].

Less extreme arid and semi-arid North American environments have been surveyed for perchlorate. Many of these have also accumulated the ion in scarcely detectable, very small amounts: for example, on the order of 1–10 μg kg^{-1} dry soil, where chloride might also be present at 3 or more orders of magnitude greater concentrations [27–30]. Considerably higher (100-fold) concentrations of perchlorate have been found in the very arid soils of the Antarctic [30]. Accumulation of the anion there may have occurred for the same reasons as in the Atacama: that is, because the land has remained extremely dry and unperturbed by either human or microbial activity [31].

The detection of perchlorate in areas where it might have remained undisturbed over long time periods suggests that there are indeed natural mechanisms for perchlorate production. These mechanisms must have been at work for at least several thousand years. Perchlorate has been detected in ground waters deposited thousands to tens of thousands years ago and in glacial ice dating as far back as 2000 years [32–34]. Results from surveys of ground water, ice, and relatively unperturbed deserts have been used to estimate a $0.1–3 \times 10^9$ kg "global inventory" of natural perchlorate presently on Earth [22, 28, 33].

Anthropogenic contributions of perchlorate to the environment are relatively recent and far less subtle. The redistribution of natural, Chilean perchlorate stowed away with the nitrate fertilizers has already been mentioned. Industrial perchlorate production from 1951 to 1997 in the U.S. has been estimated as 5×10^9 kg [22]: a figure on the same order as the Earth's entire estimated inventory of natural perchlorate. Man-made perchlorate has been used in the production of rockets, missiles, fireworks, and the like, where perchlorate's oxidizing power allows it to be used as a propellant and explosive [12]. Environmental surveys in the early 2000s identified perchlorate as a widespread contaminant in drinking water, crops, and milk, particularly in areas of the southwest United States where perchlorate had been produced or used [16, 21, 35–41]. Microbial perchlorate respiration was documented at around the same time [42, 43], and its origins were then unclear. The identification of perchlorate-respiring bacteria in non-contaminated sites and of perchlorate reservoirs in places predating human activity both suggest that natural perchlorate supplied the initial selection pressure needed for the evolution of perchlorate respiration. This suggestion has gained further support as perchlorate-reducing enzymes have been identified in both taxonomically broad and temporally ancient reaches of the tree of life (see Section 3.1.)

2.3 *Atmospheric and Extraterrestrial Origins of Perchlorate*

Natural perchlorate may be accruing on the Earth's surface, but there remains no documented geological or geochemical means of producing it. It would appear as if

perchlorate simply falls out of the sky. This suggestion is not so facetious, as the identification of perchlorate in pristine and geographically widespread ground waters, ice cores, rain, and snow indeed suggests atmospheric origins [34, 44]. Three atmospheric sources of perchlorate have been proposed:

First, laboratory experiments with simulated lightning have shown that perchlorate is produced, albeit less efficiently than nitrogen oxides, in oxygenic atmospheres in the presence of Cl^- [45]. Higher voltages and lower humidity, conditions found in high energy storms in dry locales, promote the greatest yields [45]. Second, reactions of aerosolized chlorine and oxygen species, energized by ultraviolet light, have long been known to occur. For example, perchlorate can be formed from reactions between ozone (O_3) and chloride. As a consequence, perchlorate has been proposed to be a stable sink for chloride in the stratosphere, where because of kinetic stability it is expected to resist decomposition by photolytic processes [46, 47]. Perchlorate's presence in the stratosphere has since been experimentally verified by single particle mass spectrometry on research flights at altitudes of up to 19 km [46]. Such atmospheric reactions would be a highly probable source of continuously deposited, natural, terrestrial perchlorate. Third and finally, in addition to these atmospheric sources, localized deposits of perchlorate have been proposed to have been brought to the Earth's surface by meteors [28].

2.4 *Perchlorate on Mars*

In 2008, the Phoenix Lander spacecraft, with the Wet Chemistry Laboratory (WCL) onboard, landed on the surface of Mars (Figure 2) [153]. The WCL analyzed three separate cubic centimeter soil samples for their water-soluble constituents. Quite stunningly, ClO_4^- was found to be their major anionic constituent (0.4–0.6 % by mass) [48].

Figure 2 Side-by-side images of the Martian surface (**left**) and Atacama Desert (**right**). The Martian surface is rich in perchlorate, as it lacks the action of bacteria which would otherwise eliminate it. The Atacama Desert's hyperarid interior is largely lifeless, relatively devoid of geochemical or hydrological activity, and a surrogate for Mars in NASA training missions. It is also the only place on Earth where perchlorate has accrued to a significant extent. The Martian image was taken by the Spirit rover and is courtesy of NASA/JPL-Caltech. The photograph of the Atacama Desert was freely provided by Dr. Mark Claire of the Blue Marble Space Institute of Science.

The hyperarid Martian surface environment is not unlike the Atacama Desert or the dry valleys of the Antarctic, places on earth which have served as Mars surrogates in preparation for missions and places where perchlorate has also accumulated. How Martian perchlorate is generated is not currently known. It could be produced by atmospheric processes similar to those on earth, though the source of the oxygen atoms (O_2, O_3, CO_2, H_2O) is not clear. Mineral-catalyzed photochemical processes, using chloride and water as chemical ingredients, have also been proposed and given some Earth-bound experimental support [49]. Such processes would take advantage of the intense UV light permitted by the thin ozone layer around Mars.

Even if perchlorate production on Mars occurs at a similar or even slower rate than on Earth, the complete lack of hydrological or biological forces for its removal would certainly allow for it to accrue on the Martian surface. Whether this perchlorate could or ever did serve to support Martian microbial life, whether it could serve as a chemical feedstock for O_2 production, and what it tells us about the chemistry of the Martian atmosphere are all open questions for future discussion and perhaps even experimental work.

3 Perchlorate Respiration

3.1 Diversity of Perchlorate-Respiring Microbes

The first dissimilatory (i.e., respiratory) perchlorate-reducing bacteria were isolated in 1996 [42, 43], touching off research both into natural sources of environmental perchlorate (above) and the origins of perchlorate metabolism. Since 1996, $\geq$50 strains using chlorate or perchlorate as respiratory electron acceptors [collectively, "(per)chlorate"] have been discovered (Figure 3) [50]. The overwhelming majority of these are β-Proteobacteria isolated from freshwater, mesophilic, neutral-pH environments [6, 11, 51, 52].

It has been debated whether these species encompass the real diversity of perchlorate respirers, or whether they merely reflect where the light of investigation has shone most brightly. There is some evidence that the latter phenomenon may be at work. Sampling in a marine environment, for example, yielded the first ε-Proteobacterial dissimilatory perchlorate-respiring bacterium, from the Arcobacter genus [53]. How far this metabolism extends beyond the Proteobacteria, into Gram-positive bacteria or Archaea, for example, is not clear, as the current evidence is incomplete. *Moorella perchloratireducens* and *Sporomusa* strain An4 (Gram-positives, phylum Firmicutes) were identified from an underground gas storage facility and shown to have perchlorate-reducing activity [54, 55]. Similarly, strains of *Bifidobacteria* (Gram-positives, phylum Actinobacteria) have been shown to reduce perchlorate. In each case, though reduction of perchlorate was observed, respiration of the anion has not been verified nor have the genetics of

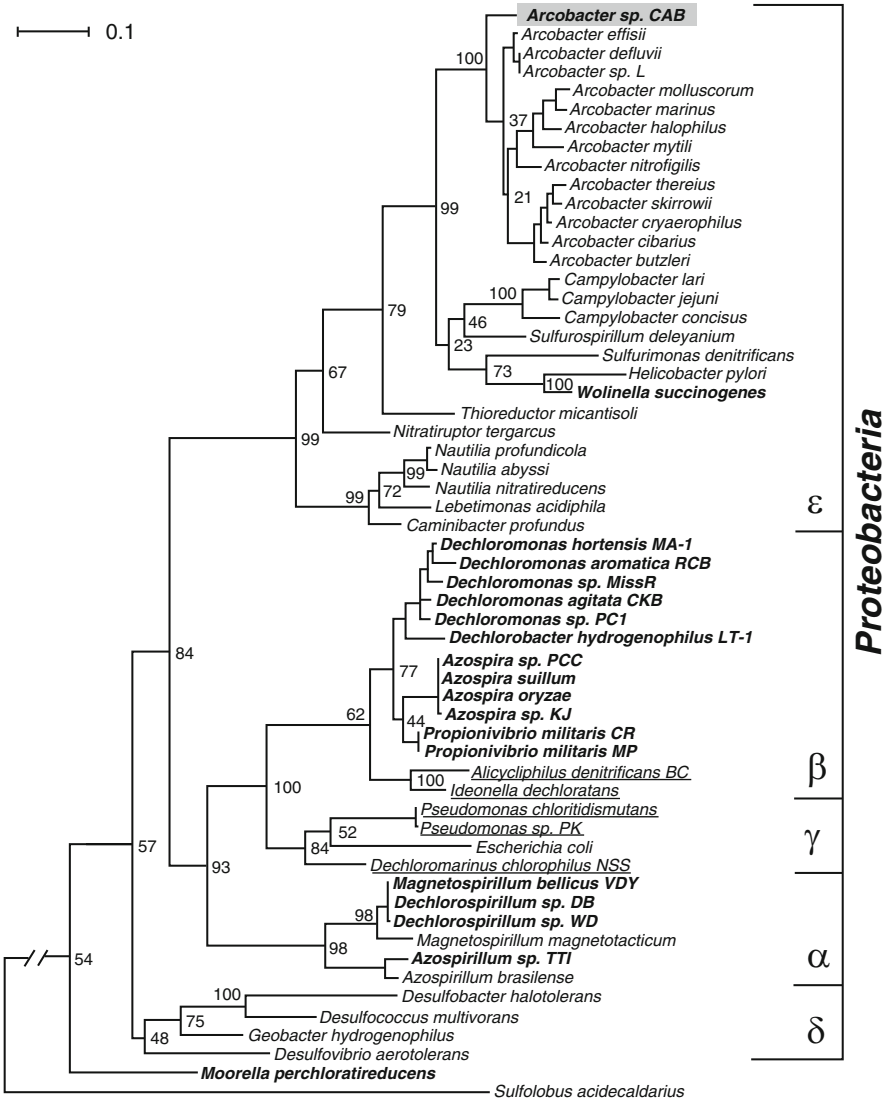

Figure 3 Diversity of characterized perchlorate- and chlorate-respiring bacteria. Maximum likelihood tree based on 16S rRNA sequences showing the phylogenetic relationships of known perchlorate (bold)- and chlorate (underlined)-reducing bacteria. Bootstrap values are based on 1,000 replications and are shown at the nodes of the tree. The scale bar represents 0.1 expected change per site [53].

reduction been probed [56]. Because the natural atmospheric events leading to perchlorate production would have existed perhaps deep in prehistory, evidence of perchlorate reduction was sought – and found – in an ancient organism. *Archaeoglobus fulgidis* is a hyperthermophilic Archaean from extreme subsurface

sulfate-reducing environments that resemble conditions on early Earth. This organism appears to possess both genes encoding a perchlorate reductase enzyme (below) and the physiological capacity to use perchlorate as a respiratory anion [57].

3.2 Genetics and Genomics of Perchlorate-Respiring Microbes

Perchlorate-respiring bacteria convert perchlorate to O_2 and Cl^- via two enzymes: perchlorate reductase (Pcr) and chlorite dismutase (Cld). Pcr is encoded by a four-gene operon (*pcrABCD*) that is functionally similar and homologous to the operon that encodes respiratory nitrate reductase (*narGHJI*) in diverse bacteria. In some cases (examples include *Ideonella dechloratans* [58] and *Pseudomonas chloritidismutans* AW-1 [59]), bacteria may respire chlorate but not perchlorate. The responsible enzyme in these organisms is consequently called a chlorate reductase (Clr). It has been experimentally shown that Pcr enzymes can reduce chlorate; however, Clr appears to be unable to reduce perchlorate. These differences in substrate specificity may reflect the far greater kinetic lability of chlorate, which can in fact be reduced by several enzymes including Nar and selenite reductase (Ser), as well as abiotically by Fe(II) or Mn(II) [60, 61]. The ultimate end products of (per)chlorate respiration are water and chlorite. Though the latter anion could in principle be further reduced to provide yet more respiratory energy, it is not reduced. Instead, it is simply detoxified, via the enzyme Cld.

In spite of the similarity of the reactions they catalyze, the Pcr and Clr enzymes are encoded by distinct genes with separate evolutionary origins. The sequences of the PcrA and ClrA subunits, where the oxochlorate anions are reduced, place both enzymes into the dimethyl sulfoxide (DMSO) reductase class (Figure 4). This class can be further subdivided into types I, II, and III, corresponding to three distinct phylogenetic clades [62]. The type I enzymes include periplasmic nitrate reductase (NapA), assimilatory nitrate reductase (NasA), and arsenite oxidase (AsoA). PcrA and ClrA are both type II enzymes, along with selenate reductase (SerA) and the dissimilatory/respiratory nitrate reductase (NarG). However, within the type IIs, the PcrA subunits form their own monophyletic group that is most closely related to the NarGs. The ClrA subunits, by contrast, are more closely related to SerA [50]. Additionally, the four Clr- and Pcr-encoding genes occur in a different order relative to one another (*pcrABCD* versus *clrABDC*), where the gene ordering is conserved between Pcr/Nar and Clr/Ser, respectively.

Genomic analyses support the conclusion that perchlorate and chlorate metabolic pathways are genetically and etiologically different, as well as primed for horizontal transfer between species. The first perchlorate-reducing organism to have its genome sequenced was *Dechloromonas aromatica* strain RCB [63]. Genome sequences for *Azospira suillum* strain PS [64], the α-Proteobacterium *Magnetospirillum bellicus* strain VDYT [52], *Dechloromonas agitata* strain CKB [63],

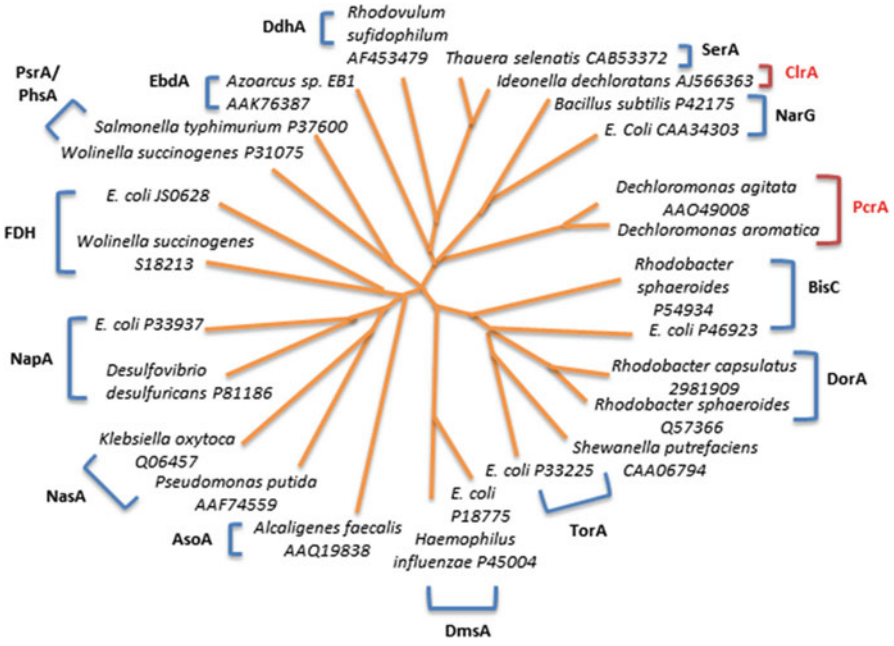

Figure 4 Unrooted neighbor-joining tree illustrating the phylogenetic relationships among type II DMSO-reductase superfamily members. GenBank accession numbers are given after the names. Based on information provided in [50].

and *Dechlorosoma suillum* PS [65] have since followed. Similarly, the genomes of five chlorate respiring bacteria (*Ideonella dechloratans*, *Pseudomonas* sp. strain PK, *Dechloromarinus chlorophilus* NSS, *Shewanella algae* ACDC [66], and *Alicycliphilus denitrificans* [67, 68]), have been sequenced [66]. Each set of genomes has been compared in order to better understand the evolutionary origins of perchlorate and chlorate metabolism, and the relationships between these two [65]. In perchlorate-respiring bacteria, the Pcr- and Cld-encoding genes are located on a genomic island. In chlorate respirers, the Clr and Cld encoding genes are on a "composite transposon," a region of the genome flanked by so-called insertion sequences. Insertion sequences are hot spots for bacterial evolution, serving as sites for homologous recombination and plasmid integration. Even among the relatively small available sample set, the transposon varies in its location (genome *versus* plasmid), copy number, and composition.

The *cld* gene in all of these organisms is, genomically speaking, something of a rogue. In perchlorate respirers, it appears to assume a number of possible orientations relative to the *pcrABCD* operon, and its transcription may be under separate regulation [69, 70]. Based on incongruence between protein and species phylogenies, *cld* genes have been predicted to have undergone horizontal transfer between species on several occasions [71, 72]. A functional chlorite-degrading chlorite dismutase protein was isolated, for example, from Candidatus *Nitrospira defluvii:* a nitrite-oxidizing bacterium without a (per)chlorate reductase and without

known (per)chlorate-respiring capabilities. Genetic evidence suggests that the *cld* gene in this species was transferred from a taxonomically distant (per)chlorate respirer. The genomic analyses described above suggest that chlorite dismutase originated in the perchlorate respiratory islands, from which it has likely been uprooted and transferred (along with peripheral genetic sequences) to the composite transposons in the chlorate respirers [66]. The movement of a *cld* gene effectively completes the chlorate respiratory pathway. Such transfers appear to have happened on more than one occasion, again even in the relatively small pool of available genomic sequences.

Some chlorate respirers may have an additional *cld* gene that is not associated with the chlorate reductase transposon. These *clds* form a lineage, sometimes called "lineage II", that is closely related to but nonetheless evolutionarily distinct from the longer, respiration-associated lineage I proteins. Additionally, Proteobacteria with no known oxochlorate respiratory pathways – for either perchlorate or chlorate – may also contain a lineage II Cld. The chemical properties and biological roles of these "Clds" are not clear and are currently under investigation (below).

3.3 (Per)chlorate Reductases

Perchlorate reductases, like nitrate reductases, are molybdenum-dependent oxo-transferase enzymes. Molybdenum in the protein's α-subunit is coordinated to the thiolates of two pterin cofactors. Each pterin, in turn, is connected to a guanine dinucleotide by a pyrophosphate linkage, and the whole cofactor is known as bis(MGD)Mo [bis(molybdopterin guanine dinucleotide)-molybdenum]. The molybdenum may additionally have a variable number of hydroxide, carboxylate, and cysteine or selenocysteine ligands. In PcrA, the protein-derived ligand is likely a conserved aspartate. Generally speaking, proteins in this family catalyze the transfer of an oxo-atom to or from a substrate. The molybdenum is the holder of two electron equivalents in this transaction, cycling between Mo^{IV} and Mo^{VI}. Hence, the complete perchlorate reductase reaction cycle is:

$$\text{bis(MGD)}Mo^{IV} + ClO_4^- \rightleftharpoons \text{bis(MGD)}Mo^{VI}{=}O + ClO_3^- \quad (7)$$

$$\text{bis(MGD)}Mo^{VI}{=}O + 2\ e^- + 2\ H^+ \rightleftharpoons \text{bis(MGD)}Mo^{IV} + H_2O \quad (8)$$

$$\text{bis(MGD)}Mo^{IV} + ClO_3^- \rightleftharpoons \text{bis(MGD)}Mo^{VI}{=}O + ClO_2^- \quad (9)$$

$$\text{bis(MGD)}Mo^{VI}{=}O + 2\ e^- + 2\ H^+ \rightleftharpoons \text{bis(MGD)}Mo^{IV} + H_2O \quad (10)$$

In respiratory pathways, reduction reaction occurs at the end of an electron transport chain. Passage of electrons to the substrate is used to generate a proton gradient and, in turn, ATP. Here, perchlorate is initially reduced in a two-electron, water-producing step to chlorate (eqs 7 and 8). A similar Pcr- or Clr-mediated two-electron step reduces chlorate to chlorite (eqs 9 and 10). The electrons in each case come from the electron transport chain embedded in the bacterial inner

membrane. These reducing equivalents ultimately originate from a variety of carbon sources that the (per)chlorate-respiring bacteria use as food.

The molybdopterin active site is housed in the α-subunit of Pcr, Clr, or Nar, encoded by PcrA, ClrA or NarG, respectively. Though the subunits are homologs, PcrA or ClrA are considerably smaller (60–104 kDa *versus* 104–150 kDa) and hence distinct from NarG, making it possible to predict from the sequence (even without computational analysis) that an operon could be involved in oxochlorate metabolism. PcrA- and ClrA-encoding genes moreover begin with a twin-arginine signal peptide, which target the Pcr and Clr enzymes for transport to the periplasmic space in their folded form.

The PcrA, ClrA, and NarG subunits interface with a second, iron-sulfur cluster containing a β-subunit, encoded by *pcrB*, *clrB*, or *narH*. The purpose of the β-subunit is to relay electrons from the respiratory electron transport chain to the α-subunit. Clr and Nar have a further, heme-containing γ-subunit (*clrC, narC*) that anchors the whole complex to the inner membrane and serves as an electron conduit (Table 1). Pcr, by contrast, appears to be a freely diffusing periplasmic enzyme. Electron equivalents originating from the membrane are predicted to reach the FeS clusters through a soluble, cytochrome *b*-containing γ-subunit (*pcrC*) and electron transporting mediators [73].

Table 1 Characterized chlorate and perchlorate reductases.

Organism	Known electron acceptors	Pcr or Clr subunits	Cofactors	Ref.
Azospira oryzae GR-1	ClO_4^-, ClO_3^-, NO_3^-, IO_3^-, BrO_3^-, Mn(IV), O_2	$\alpha_3\beta_3$	Mo, FeS	[43, 151]
Strain Perc1ace	ClO_4^-, NO_3^-	$\alpha_3\beta_3$		[146]
Azospira sp. KJ	ClO_4^-, ClO_3^-, O_2	αβ		[147]
Ideonella dechloratans	ClO_4^-, NO_3^-, IO_3^-, BrO_3^-, O_2	αβγ		[153, 154]
Pseudomonas sp. PDA	ClO_3^-, O_2	αβγ	Mo, FeS, heme *b*	[147]
Pseudomonas chloritidismutans	ClO_3^-, O_2	αβγ	Mo, FeS	[148]

Adapted from [70].

Finally, the δ-subunit of each of these protein complexes (encoded by *pcrD*/*clrD*) is a chaperone involved in maturation of the enzyme and possibly in insertion of the bis(MGD)Mo cofactor.

3.4 Chlorite Dismutases and Perchlorate Respiration

All bacteria with a functional Pcr or Clr have a *cld* gene that encodes a *bona fide*, functioning chlorite dismutase: that is, a protein that detoxifies chlorite by converting it to Cl^- and O_2. In the absence of this reaction or some other means

of eliminating chlorite, this end product would accrue to a toxic level. Interestingly, the only known perchlorate-respiring Archaean, *A. fulgidis*, is able to overcome chlorite toxicity even though it lacks a *cld* gene. How *A. fulgidis* degrades chlorite is not known, but abiotic means have been proposed.

The gene encoding the respiration-associated Cld, as described above, is near to the *pcrABCD* or *clrABDC* operon but not necessarily in a static location [66]. The properties of these O_2-generating proteins are described in detail in Section 4. Notably, many species with no known (per)chlorate metabolism possess a *cld* gene. Current evidence suggests that these non-respiratory Clds are not efficient detoxifiers of chlorite and that they serve other cellular roles, as discussed below.

4 Oxygen Generation by Chlorite Dismutases

4.1 Structures

4.1.1 Primary Structures: Diversity and Hallmarks of O_2 Generation

For an organism to respire chlorate/perchlorate, some means of chlorite degradation is necessary because chlorite is toxic. However, the presence of a *cld* gene does not correlate with either the possession of (per)chlorate reductase encoding genes, or with the ability to reduce oxochlorates. The "lineage I" and "lineage II" Clds were described above as two closely related but distinct groups of *cld* genes found thus far primarily in Proteobacteria. When a rainbow of microbial genome sequences began to emerge in earnest in the early 2000s, *cld* genes could be found in a great number of them. In fact, *cld*-family genes have been identified in highly diverse microbes from at least 9 bacterial and 2 archaeal phyla (Figure 5) [71]. They cluster into at least three additional monophyletic sequence groups beyond lineages I and II.

The respiration-associated Clds come from lineage I, and these proteins all rapidly emit O_2 when presented with chlorite (Figure 6, Table 2). The well-studied Cld from *Dechloromonas aromatica* (*Da*Cld) survives an impressive 20,000 turnovers with this often-punishing oxidant before its heme irreversibly lyses. By contrast, Clds from diverse bacteria beyond the Proteobacterial phylum – for example, *Staphylococcus aureus* (Gram-positive pathogen, phylum Firmicutes) and *Thermus thermophilus* HB8 (Gram-negative hyperthermophile, phylum Deinococcus-Thermus) have no and very little chlorite-degrading capacity, respectively, and their parent organisms do not respire oxochlorates [74, 75]. So, do all Clds from non-respirers fail to produce O_2? Not exactly. Clds from two nitrite-oxidizing, non-(per)chlorate-respiring bacteria were shown to convert chlorite to dioxygen [71, 76], and they illustrate two known types of exceptions. The first of these, the Cld from Candidatus *Nitrospira defluvii,* is clearly a lineage I Cld that appears to have arrived in the *N. defluvii* genome via horizontal transfer from a perchlorate respiring organism. The environmental selection pressures promoting its transfer and retention in its new host are not yet understood. The second of these is the Cld from *Nitrobacter winogradskyi*, which is representative of the lineage II

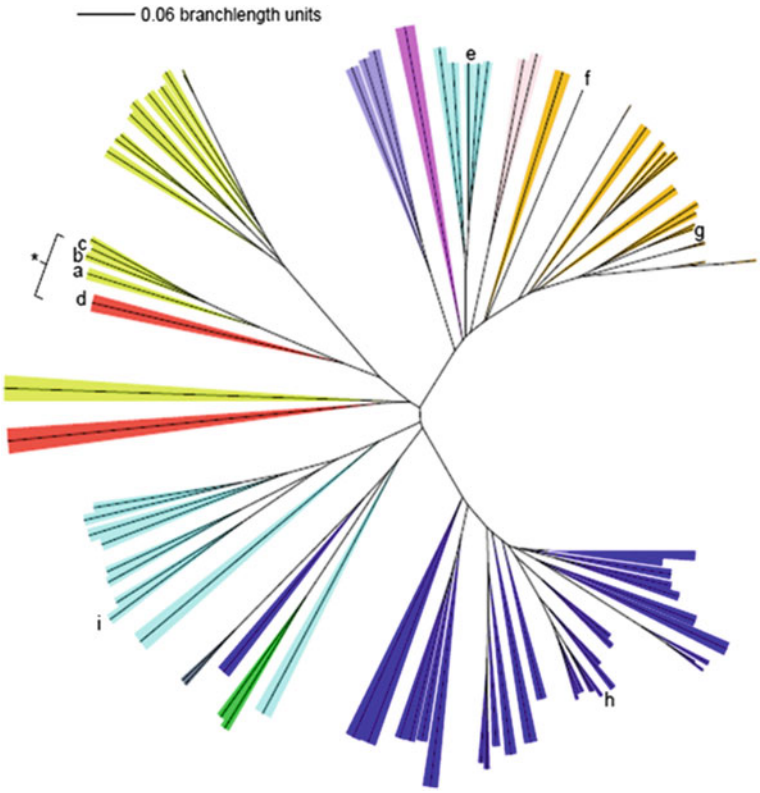

Figure 5 Phylogenetic trees illustrating the diversity of Cld sequences. The phylum/kingdom affiliation of each species is indicated by color: Proteobacteria (yellow), Firmicutes (orange), Nitrospirae (red), Actinobacteria (blue), Archaea (light blue), Deinococcus-Thermus (grey), Chloroflexi (green), Planctomycetes (dark purple), Veruccomicrobia (light purple), and Acidobacteria (pink). The Halobacteriacea, pictured near the bottom of the tree, form their own group distinct from the other archea. Species known to carry out chlorite detoxification are indicated with a bracket/asterisk. Clds from several species are designated with letters: (a) *Dechloromonas aromatica*; (b) *Dechloromonas agitata*; (c) *Ideonella dechloratans*; (d) *Nitrospira defluvii*; (e) *Halobacterium* sp. NRC-1; (f) *Thermus thermophilus* HB8; (g) *Geobacillus stearothermophilus*; (h) *Mycobacterium tuberculosis*; (i) *Thermoplasma acidophilum*. A three-iteration protein similarity (PSI-BLAST) search was performed using *Da*Cld as the bait sequence. The top 500 result sequences were aligned by ClustalX, and a phylogenetic tree was constructed. Representative sequences from each phylum were chosen for the above display. Settings used for the tree building were: random number = 111 and bootstrap maximum = 1000. The iTOL (Interactive Tree of Life) program was used for branch coloring and figure generation (http://itol.embl.de/). Reproduced with permission from [83]; copyright 2011 Elsevier.

Clds that are found predominantly or perhaps exclusively in Proteobacteria. Though the lineage II *clds* occur in genomes independently of (per)chlorate reductase genes, the *N. winogradskyi* Cld and potentially other members of this group (including the Cld from the pathogen *Klebsiella pneumoniae*) can produce O_2 from chlorite. The number of turnovers sustained before the heme is irreversibly destroyed,

however, is sharply limited. Hence, while chlorite catalysis is observable, the catalyst is not robust, suggesting that chlorite decomposition may not be the biological function of the lineage II proteins.

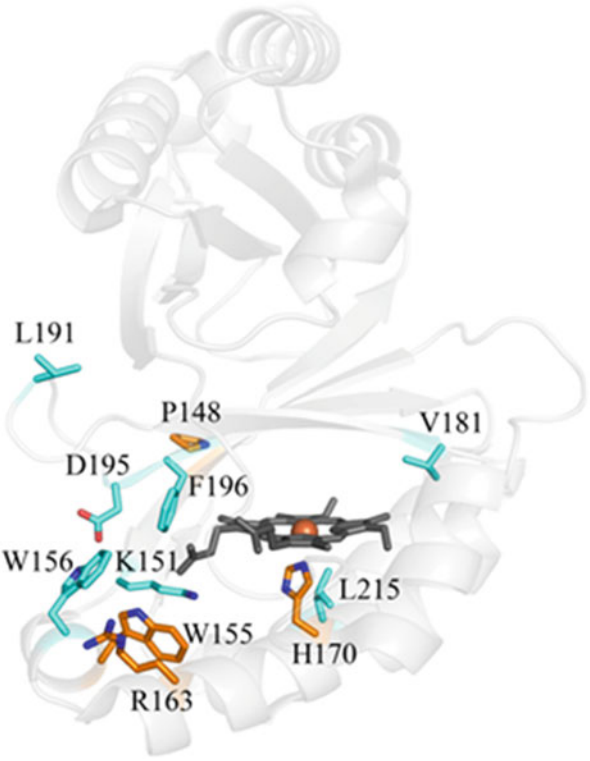

Figure 6 *Da*Cld monomer structure showing the locations of residues conserved among Clds from taxonomically diverse sources. The *Da*Cld monomer is shown as a faded gray cartoon. Strictly (carbon orange) and strongly (carbon cyan) conserved residues are shown as sticks and colored by atom (carbon orange and cyan, respectively). Heme is drawn in gray stick, and the iron is drawn as an orange sphere. All conserved residues fall within the C-terminal domain. This figure was generated using PyMOL (http://www.pymol.org/). Figure reproduced with permission from [83]; copyright 2011 Elsevier.

Table 2 Kinetic constants for the steady state reaction of chlorite dismutases.

Organism	k_{cat} (min^{-1})	K_M (μM)	k_{cat}/K_M ($M^{-1}\ s^{-1}$)	Temp. (°C)	pH[a]	Ref.
Dechloromonas aromatica	4.5×10^5	210	3.5×10^7	4	6.8	[98]
Ideonella dechloratans[b]	1.6×10^5	150	1.8×10^7	25	7.0	[149]
Ideonella dechloratans[c]	1.1×10^5	260	7.1×10^6	25	7.0	[150]
Strain GR-1	7.2×10^5	170	7.1×10^7	30	7.2	[145, 151]
Pseudomonas chloritidismutans AW-1	1.4×10^4	80	2.7×10^6	25	6.0	[152]
Thermus thermophilus HB8	4.6×10^1	12,000	5.9×10^1	25	7.0	[74]
Candidatus Nitrospira defluvii	2.1×10^3	58	6.0×10^5	30	7.0	[82]
Nitrobacter winogradskyi	1.1×10^4	90	2.1×10^6	30	7.0	[76]

[a]All reported measurements made in varying concentrations (10–100 mM) of phosphate buffers.
[b]Heterologously expressed in *E. coli*.
[c]Purified from native organism.

This conclusion is consistent with the lack of a known biological imperative for chlorite detoxification by their parent organisms, although it is possible that these Clds catalyze detoxification of chlorite produced by Nar-mediated chlorate (ClO_3^-) reduction. In short, the available evidence suggests that only the respiration-associated Clds – encoded by genes on perchlorate reductase islands or composite transposons near *pcrABCD*/*clrABDC* operons, or recently mobilized from such – efficiently convert chlorite to O_2 and Cl^-. Cld homologs from outside this relatively small group are biochemically distinct and appear to serve other biological roles.

Sequence alignments including lineage I, II, and the more taxonomically broad Clds show that the family as a whole is quite sequence-diverse (Figure 7, Table 3). Only three amino acids are strictly conserved family-wide. These include the proximal histidine ligand to the heme iron (H171 in *Da*Cld, with residue numbering reflecting the structurally characterized mature form of the protein lacking the SecB tag earmarking the protein for secretion to the periplasm) [4]. They also include a tryptophan near the porphyrin binding site (Trp155) and a proline residue important for maintaining the protein's fold (Pro148). This sequence diversity, the taxonomic breadth of organisms containing the gene, and the presence of several monophyletic groups of Clds suggests an ancient origin for *cld* in which divergence of the sequence occurs at pace with speciation events. The exception to this pattern comes, of course, for the heavily traveled *cld* genes associated with oxochlorate respiration [65, 66, 71, 77].

What sequence features distinguish the O_2-generating Clds from their non-O_2-generating counterparts? There are at least three (Figure 7, Table 3). First, in oxochlorate-respiring bacteria, the Cld-encoding sequence is preceded by a SecB peptide, signaling transport of the protein to the periplasm in its unfolded, heme-free form. Clds from the non-respirers, by contrast, are cytoplasmic. Second, both the longer lineage I Clds from oxochlorate respirers and the shorter lineage II Clds share a conserved arginine residue in the pocket above the heme plane. Proteins from each of these groups have been experimentally confirmed to produce O_2 rapidly, even if the lineage I proteins are considerably more robust (i.e., higher numbers of turnovers). The distal Arg residue is not conserved in the various non-O_2-producing branches of the phylogeny depicted in Figure 5, changing for example to serine (Euryarchaeota), glutamine (Firmicutes), or asparagine (Actinobacteria). Surprisingly, the arginine can be mutagenically substituted with an asparagine in *Da*Cld without completely abrogating activity with chlorite [78]. However, the Cld from *Staphylococcus aureus* (phylum Firmicutes), which has a distal glutamine residue in the analogous position, has no measurable chlorite-degrading activity. Finally, a second tryptophan near the heme's periphery (Trp156) and two residues from a triad of hydrophobic amino acids above the heme plane (Leu185 and Phe200) are strictly conserved among all Clds. The tryptophan appears to be critical for maintaining the bound heme as well as the protein's oligomeric state [79], and hydrophobicity in the distal pocket may be essential for stabilizing reaction intermediates (see Section 4.2.)

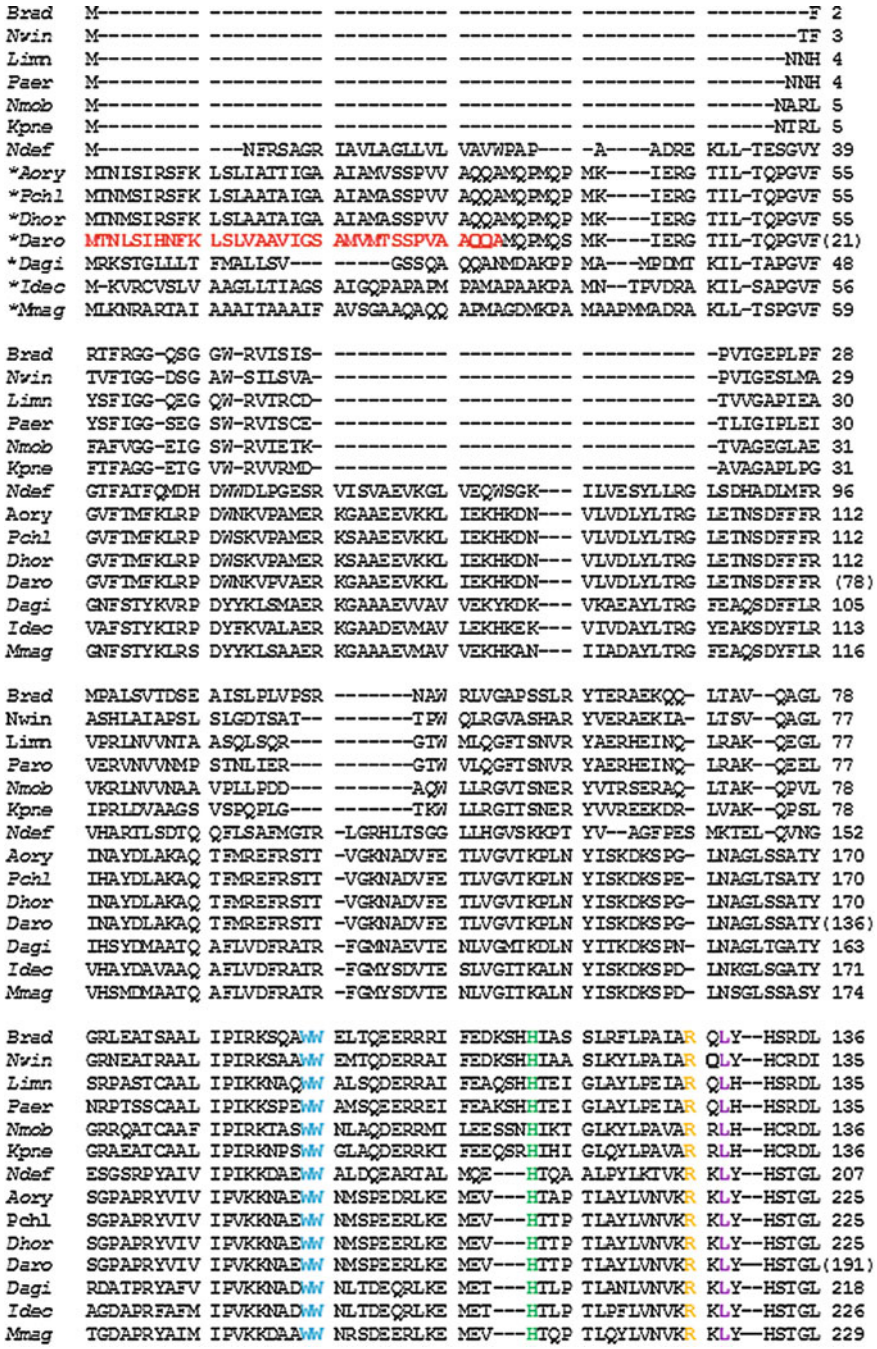

Figure 7 Structure-based sequence alignment of O_2-emitting Cld sequences, from perchlorate respirers and short Proteobacterial Clds with confirmed chlorite decomposition activity. Experimentally confirmed respiratory Clds are indicated with an asterisk by the species name. The proximal histidine-glutamic acid pair is highlighted in green, the conserved distal arginine in yellow, and the distal hydrophobic triad in purple, and the conserved pair of tryptophans and a proline residue are in blue.

Fig. 7 (continued) The SecB-dependent secretion peptide sequence on the Cld sequence from *D. aromatica* (*Daro*) is shown in red. Sequence numbering with this peptide removed is shown in parentheses. The species names are abbreviated as: *Bradyrhizobium* sp. S23321 (*Brad*), *Nitrobacter winogradskyi* (*Nwin*), *Limnobacter* sp. MED105 (*Limn*), *Pseudomonas aeruginosa* (*Paer*), *Nitrococcus mobilis* (*Nmob*), *Klebsiella pneumoniae* (*Kpne*), Candidatus *Nitrospira defluvii* (*Ndef*), *Azospira oryzae* (*Aory*), *Pseudomonas chloritidismutans* (*Pchl*), *Dechloromonas hortensis* (*Dhor*), *Dechloromonas aromatica* (*Daro*), *Dechloromonas agitata* (*Dagi*), *Ideonella dechloratans* (*Idec*), *Magnetospirillum magnetotactica* (*Mmag*).

Table 3 Conservation of residues of likely functional relevance among the Clds.

Amino acid[a]	Proposed role	Oxochlorate-respiring bacteria[b]	Firmicutes	Euryarchaeota	Actinobacteria
H170	Proximal heme ligand	conserved	conserved	conserved	conserved
Elu220	H-bonding to axial His	conserved	conserved	K, R, M, L, E	variable
R183	distal polar residue	conserved	Q	S	A, Q[c]
L185	distal hydrophobic triad	conserved	I	T	L, I, or T
T198	distal hydrophobic triad	conserved	V, T	V	T, V, or L
F200	distal hydrophobic triad	conserved	L, F	Y	variable
W155	radical pathway	conserved	conserved	conserved	conserved
W156	radical pathway	conserved	Y	Y	W, T
H224	radical pathway	mostly conserved	R	W	variable
W227	radical pathway	mostly conserved	E	variable	variable
Dsp192	Ca^{2+}ligand	conserved	G	variable	D, G
T231	Ca^{2+}ligand	conserved	F	I, L, V	variable

[a]The residue numbering shown here refers to the structurally characterized, mature *Da*Cld with its SecB signal peptide removed.
[b]Includes sequences from all experimentally verified oxochlorate respirers.
[c]The residue at this position in alignments is A, but is adjacent to a conserved Q.

4.1.2 Heme-Binding Domain

The heme-binding domain of Clds consists of a series of α-helices lining the proximal side of the heme plane and a row of β-sheets over the distal, open coordination position. The iron is ligated by a histidine residue that is strictly conserved throughout the Cld family (Figure 6). In the full length Clds – that is, all Clds except those in lineage II – the protein monomer contains two mutually homologous domains, each about 140 amino acids in length. These resemble one another in secondary structure, with the exception of an added α-helix in the N-terminal domain, and are linked by a pseudo twofold axis of symmetry. The extra helix, the lack of a strictly conserved histidine, and a slightly more compact structure may be responsible for the failure of heme to bind in the N-terminal domain [4, 76, 80–82].

Heme is typically found in predominantly α-helical environments, such as in the globins, cytochrome P450, catalases, and peroxidases. Hence, the Cld heme-binding domain at first seemed somewhat unusual. However, it is now clear that the mixed α-helical/β-sheet domain of Clds is shared by a very large structural superfamily of proteins, many of which derive from microbes and only a small fraction of which associate with heme [75, 83]. Subfamilies range from quite close to Clds in sequence (and therefore ancestry) to relatively distant. At least two subfamilies in addition to the Clds are known to interact with heme. They are catalytically dissimilar to Clds, in spite of their identical heme-binding architecture and mutually conserved residues in the active site. The first subfamily contains the bacterial IsdG-type heme oxygenases that oxidatively cleave heme as a substrate, releasing the iron for cellular use [84]. Unlike Clds, the IsdG-family proteins have just one domain per monomer. Two heme-binding monomers come together to form a dimer that resembles the *Da*Cld bidomain monomer [85]. The heme in IsdI (from *Staphylococcus aureus*) also assumes a different orientation than in the Clds and is significantly distorted from planarity. Structural distortion of the tetrapyrrole is known to be important for catalysis [86].

The dye-decoloring peroxidases (DyPs) from bacteria and fungi form a second, diverse subfamily. These proteins are evolutionarily quite distant from the Clds, sharing as low as 6 % identity [83]. However, they are structurally very similar, having the same bidomain monomer in which only the C-terminal domain binds heme [87]. In the DyPs, however, the heme is flipped relative to its orientation in the Clds, placing its propionic acid side chains in a very different chemical environment. This again illustrates the remarkable versatility with which this protein domain is known to interact with heme [83]. One of the propionates is able to form a hydrogen bond to the conserved distal arginine. These features and the presence of a distal aspartic acid distinguish the DyPs from the Clds and may be important for their distinct chemistry [87, 88]. DyPs efficiently activate H_2O_2 to form high-valent iron-oxo intermediates which catalyze the one-electron oxidation of substrates. Clds do not, likely because they lack a base for deprotonating H_2O_2 and thereby activating it for binding to Fe(III) [89].

4.1.3 Active Site

Like heme proteins that mediate O_2 transport [90], gas sensing [91–95], and peroxidase catalysis, Clds have a proximal histidine ligand to the heme (Figure 8, left). A glutamic or aspartic acid forms a hydrogen bond to the proximal histidine's other, unligated nitrogen. Such hydrogen bonding is expected to increase the anionic (histidinate) character of the ligand in peroxidases, making the Fe(III) iron more electron-rich and therefore capable of donating significant electron density toward scission of a peroxide ligand in *trans* [96, 97]. However, resonance Raman shows that the histidine ligand in Clds, like in the gas-binding proteins, is neutral in character [98]. Also on the proximal side of the heme plane are two tryptophan residues, one strictly conserved throughout the entire Cld family (W155, *Da*Cld numbering) and the other conserved among O_2-producing lineage I Clds and related Clds from lineage II (W156). A third tryptophan (Trp227) is not strictly conserved, but is connected to the proximal histidine through a hydrogen bonding network. Finally, two tyrosine residues (Tyr118, Tyr177) are conserved among the lineage I and II Clds. Tyr118 is connected to a propionate side chain of the *Da*Cld heme by a hydrogen bond. From a structural perspective, either Tyr118 or Trp227 have a direct conduit to the heme and could therefore in principle stabilize radical intermediates, as described below.

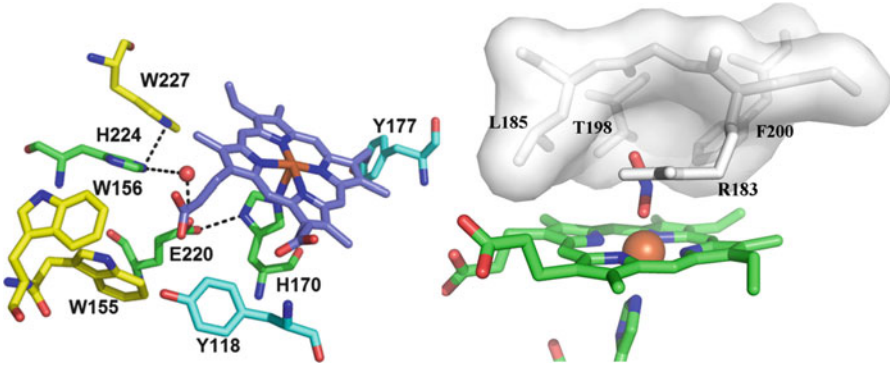

Figure 8 Structure of the proximal and distal sides of the heme in *Da*Cld. (**Left**) Proximal pocket with hydrogen bonding interactions indicated by dashed lines. A water molecule is clearly discernable even at low resolution and is represented as a red sphere. (**Right**) Residues lining the distal pocket are shown as white sticks with a transparent surface, except for Arg-183. Figures were originally generated using PyMOL (http://www.pymol.org/) from PDB 3Q08 using PyMOL and are adapted from [78] and [4].

The distal side of the heme plane (Figure 8, right) has several unique and likely functionally important features. Notably, there are no distal basic residues (histidine, aspartate, glutamate) in any of the Clds. A distal base is essential for rapid H_2O_2 activation in the well-studied peroxidases [99–101]. As mentioned above, there is instead an arginine directly above the heme plane of all lineage I and II Clds, changing to a serine or glutamine in most other Clds. This residue has no amino acid hydrogen-bonding partner in *Da*Cld or in any available crystal

structures of O_2-evolving Clds, and is instead found hydrogen-bonded to the Fe(III) heme ligand (water/hydroxide, nitrite, thiocyanate). Adjacent to the distal arginine are three hydrophobic residues: Leu185, Thr198, Phe200. Although the exact identity of the residues can vary, a hydrophobic triad is strictly conserved at these positions. They form a low, hydrophobic ceiling above the porphyrin plane in what is overall a fairly hydrophobic pocket.

While all chlorite-degrading Clds that have been crystallographically characterized also have a heme bound, a few from non-chlorite-degrading species have been characterized in their heme-free, apo forms (Table 4). These were prepared mainly by structural genomics consortia, and hence the protein expression/purification conditions may not have supplied sufficient heme. However, it has also been observed that the Cld from *Staphylococcus aureus*, which does not convert chlorite to O_2, binds heme with very low affinity and is actually somewhat difficult to prepare in a heme-bound state [75]. Intrinsically low affinity may be responsible for the failure to capture the Cld structures in the heme-bound form. By the same token, it is notable that these proteins are stable enough to form crystals in the apo/heme-free form, though solution measurements have indicated that the apo-Clds from *N. winogradskyi* and Candidatus *N. defluvii* are more prone to denaturation than their holo-counterparts [102, 103].

Table 4 Some available X-ray crystal structures for chlorite dismutases.

PDB ID	Source	Description	Ref.
3Q08	*Dechloromonas aromatica*	Nitrite-bound Cld from a PRB[a]	[4]
2VXH	*Azospira oryzae*	Thiocyanate-bound Cld from a PRB	[8]
3NN2	Candidatus *Nitrospira defluvii*	Cyanide-bound chlorite-reactive Cld from an evolutionarily distant NPRB[a]	[82]
3QPI	*Nitrobacter winogradskyi*	Water-bound short dimeric Cld from a proteobacterial NPRB	[76]
1T0T	*Geobacillus stearothermophilus*	Heme-free Cld from NPRB (Firmicutes)	[b]
1VDH	*Thermus thermophilus HB8*	Heme-free Cld from NPRB (Firmicutes)	[74]
3DTZ	*Thermo acidophilum*	Heme-free Cld from NPR-Archaeon (Euryarchaeota)	[b]

[a]PRB = perchlorate respiring bacterium, NPRB = non-perchlorate-respiring bacterium;
[b]Unpublished structure deposited in the Protein Data Bank.

4.1.4 Tertiary Structures and Oligomerization States

We conclude the discussion of Cld structures by noting the diversity of oligomerization states in which the Cld domain can be found in X-ray crystal structures. All full-length Clds (whether or not they catalyze the chlorite decomposition reaction) form a biochemically unusual homopentameric structure in which the heme-binding domains associate with each other along one face of the pentamer (Figure 9a). Uniquely in *Da*Cld, each monomer-monomer interface has a Ca^{2+} ion ligated by a strictly conserved aspartic acid (Asp192). The pentameric

shape of the complex leaves an open, solvent-filled channel in the middle of the protein, the function of which (if any) is not clear. It is also unknown whether the pentameric form is physiologically relevant, although it represents the stable solution state of the pure protein. Full-length Clds in the pentameric state with heme bound and a conserved arginine in the distal pocket are moreover the most efficient catalysts in the conversion of chlorite to O_2 and Cl^- [103].

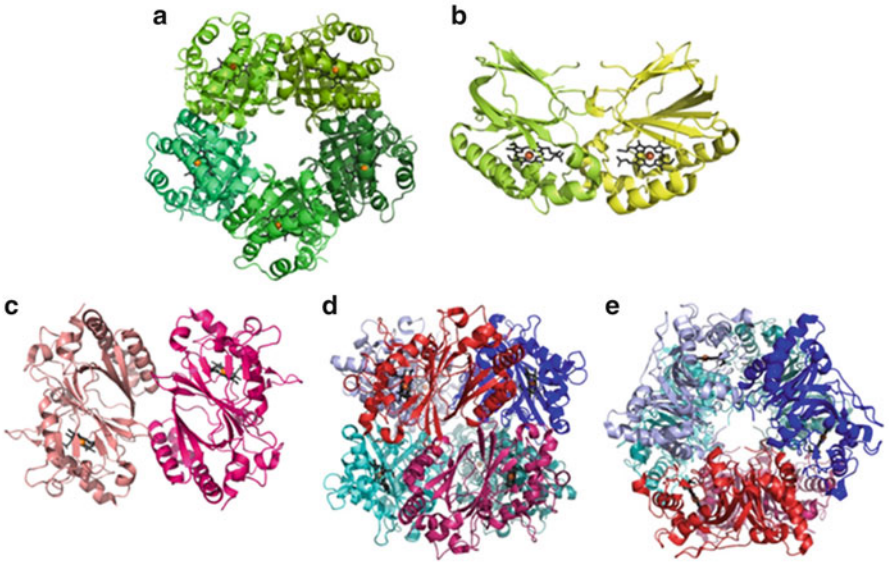

Figure 9 Biological oligomers of (**a**) *Da*Cld, (**b**) *Nitrospira winogradskyi* Cld, (**c**) TyrA from *Shewanella oneidensis*, and (**d**, **e**) DyP from *Rhodococcus jostii*, illustrating the diversity of multimeric structures assumed by structurally similar monomers in this superfamily. The monomers are individually colored, and the hemes are drawn in grey stick, with the iron as an orange sphere. Panel (**e**) is a 90° rotation of (**d**) towards the viewer about a horizontal axis. This figure was generated using PyMOL and reproduced with permission from [156]; copyright 2013 World Scientific Publishing Co.

By contrast, the short-length Cld from *N. winogradskyi* crystallizes as a dimer with a completely different monomer interface (Figure 9b) [76, 82]. This leaves the heme significantly more solvent exposed than in the pentameric structures (Figure 9a). The more open active site may be responsible for the significantly lower stability of the protein's heme. Though *Nw*Cld is capable of producing O_2 from chlorite, catalysis is limited by chlorite-dependent degradation of the heme, which appears to occur at much smaller concentrations of chlorite than in *Da*Cld.

The bacterial heme oxygenases (IsdG, IsdI) and DyPs share the heme binding domain structure of Clds but, as described above, are significantly different in sequence. The bidomain DyPs, unlike Clds, furthermore form head-to-tail dimers, where the C-terminal heme domain of one monomer interacts structurally with the N-terminal heme-free domain of the other. DyP structures may form independent dimers (Figure 9c) or a crystallographic trimer-of-dimers (Figure 9d and e).

By contrast, the monodomain IsdG-like proteins form independent dimers in which both monomers bind heme.

This diversity of oligomeric structures demonstrates that the heme-binding domain is structurally capable not only of accommodating heme in multiple orientations, but of interacting in a variety of different ways with partner proteins. Such intrinsic flexibility in their protein-protein interactions could be important for the biological functions or technological applications of diverse Clds.

4.2 Reactivity and Mechanism

4.2.1 Diversity of Reactions Catalyzed by Chlorite Dismutases

Clds catalyze at least three reactions: O–O bond formation, one-electron oxidations (peroxidase chemistry), and heme oxidation.

O–O bond formation from chlorite is the principal reaction catalyzed by full length Clds from (per)chlorate-respiring bacteria. As described above, these "*bona fide*" Clds are characterized by their pentameric oligomerization state, bidomain monomer structure, and possession of a distal pocket arginine in the heme-binding domain. They constitute a relatively small minority of all the sequenced Clds from taxonomically diverse sources. The small dimeric Clds have nearly the same active site structure as their pentameric homologs, including the distal arginine and the surrounding hydrophobic residues. These Clds also catalyze rapid O–O joining in spite of the lack of a known biological imperative by their host organisms for eliminating chlorite. However, the limited number of turnovers their hemes can sustain suggests that chlorite may not be their natural substrate [76, 104].

Whether short or long, the O_2-producing proteins also appear to be capable of catalyzing peroxidase-type one-electron oxidation reactions when either H_2O_2 or a peracid is the oxidant [89, 104]. A complete peroxidase reaction cycle has been documented for *Da*Cld, as described below. Catalysis of this reaction is very slow and the number of achievable turnovers per heme limited, consistent with the assumption that peroxidase chemistry is not the biological function of these Clds. Studies of the peroxidase reaction nonetheless have shed light on the basic chemical and biological capabilities of Clds and are therefore of interest [89].

Finally, Clds, like many heme-dependent oxidation catalysts, facilitate the oxidant-dependent degradation of their own hemes. The redox-stability of the heme in Clds is extraordinarily variable. *Da*Cld sustains ~20,000 turnovers with chlorite, per heme [105]. The dimeric Cld from *Klebsiella pneumoniae* sustains only ~2–3,000 turnovers under similar conditions [104]. The heme in the Cld from *Staphylococcus aureus* is completely destroyed by less than five equivalents of chlorite, without measurable production of O_2 [75]. Whether heme destruction serves a biological function in any of these proteins is not clear. However, it does seem to be the principal catalytic pathway followed by the *S. aureus* Cld (and likely by related pentameric Clds from non-oxochlorate-respiring bacteria) in the presence of a series of oxidants (chlorite, H_2O_2, peracids).

4.2.2 Possible Pathways for O–O Formation

There are a number of possible pathways for O_2 production from chlorite. Early efforts with *Da*Cld truncated the list by demonstrating that (i) O_2 is produced stoichiometrically with ClO_2^- degraded [105]; (ii) all of the emitted O_2 derives from chlorite, even in the presence of ^{18}O–labeled water [106]. These results strongly favored mechanisms where the two oxygen atoms of O_2 derive from the same molecule of ClO_2^-. Alternative mechanisms where chlorite acts as an oxygen atom or one-electron donor to the Fe(III) heme produce highly protein-reactive leaving groups (ClO^-, ClO_2) [107, 108] that would have to re-react quantitatively at the heme site to maintain the observed $1ClO_2^-:1O_2$ stoichiometry. They would moreover have to do so without undergoing exchange of their oxygen atoms with $^{18}OH_2$. Hence, the four possible mechanisms by which a single molecule of chlorite can be effectively rearranged to generate Cl^- and O_2, depicted in Figure 10, are preferred.

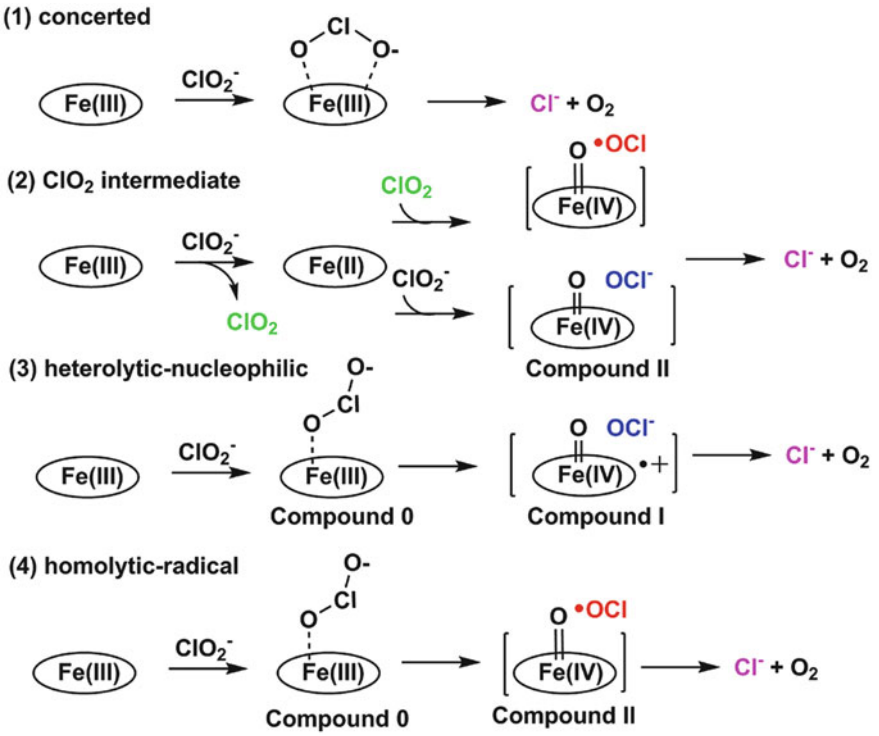

Figure 10 Possible mechanisms for O_2 formation from chlorite: (1) concerted, (2) chlorine dioxide intermediate, (3) heterolytic Cl–O cleavage/nucleophilic O–O formation, (4) homolytic Cl–O cleavage/radical O–O formation.

In pathway (1), a single molecule of chlorite binds Fe(III) in a bidentate, η^2 mode, and formation of O_2 occurs in a concerted fashion without any intermediate transfer of electrons or atoms to the iron. In pathway (2), electron transfer from

chlorite to the Fe(III) heme, depicted here as an inner-sphere process, yields the Fe(II) porphyrin and chlorine dioxide (ClO_2). This reaction (eqn. 11) is thermodynamically favorable [109] and known to be catalyzed by certain synthetic metalloporphyrins (described below):

$$ClO_2^- \rightarrow ClO_2 + e^- \qquad E^\circ = -0.934\ V \tag{11}$$

Oxygen atom transfer from chlorine dioxide to the Fe(II) iron would yield a ferryl (Fe^{IV}=O) heme. This could recombine with the released chlorine oxide to make a formally Fe(III)-$OOCl^-$ species, spontaneously breaking down to yield Cl^- and O_2. The Fe(II) Cld may also react with chlorite to give O_2, which is also depicted in Figure 10.

Pathways (3) and (4) both begin with the formation of a Fe(III) heme/chlorite complex. This complex is analogous to the Fe(III)-peroxy species (Fe(III)-OOH) formed as the initial intermediate in peroxidase reactions, known as Compound 0 [110]. The distal histidine of classical peroxidases removes the proton from H_2O_2 ($pK_a = 12$) to yield the peroxy anion, which binds avidly to Fe(III). Because the hypochlorous acid/chlorite pK_a is quite low (1.72), base catalysis would not be needed to form the analogous Fe(III)-chlorito complex.

Donation of two electrons from the Fe(III) heme leads to heterolytic scission of the coordinated O–Cl bond (pathway 3) and formation of a formally Fe(V)=O intermediate. This intermediate, observed pervasively in biological heme chemistry, is known as Compound I. Electronically, it is described as a ferryl (Fe(IV)=O) that is exchange-coupled to a radical on the non-innocent porphyrin ligand. Because loss of an electron occurs without concomitant loss of a proton, the resulting porphyrin radical is a cation (porphyrin$^{\bullet+}$). Unlike the parent tetrapyrrole, porphyrin$^{\bullet+}$ is not aromatic. Hence, the porphyrin's visible Soret absorbance band is significantly diminished in intensity in porphyrin$^{\bullet+}$, providing a simple indicator of the possible presence of Compound I. The oxygen atom in Compound I is capable of removing electrons or an electron/proton pair (hydrogen atom) from a substrate, thereby becoming reduced to the ferryl-porphyrin intermediate (Fe(IV)=O or Fe(III)-OH), also known as Compound II [111]. A good nucleophile may also attack the electron-deficient oxygen of Compound I. The oxygen atom of hypochlorite, particularly in its anionic/deprotonated form, is nucleophilic and could attack Compound I to yield the same Fe(III)-peroxychlorite intermediate proposed in pathway (1).

Alternatively, the Fe(III)-chlorite complex could react in a one-electron fashion to give the products of heterolytic O–Cl bond cleavage: Fe(IV)=O and the $ClO^\bullet$ (chlorine monoxide) radical. These two would need to re-react, once again to form a Fe(III) species with an O–O(Cl) bond (pathway 4). Chlorine monoxide is presumably a highly reactive species, perhaps not dissimilar to the hydroxyl radical. It has been described in atmospheric chemistry models but is not a known biological molecule.

There is no precedent for pathway (1) using either synthetic or biological catalysts. In fact, there are very few reported crystal structures for metals bound to chlorite, and none in either the through chloride or bidentate O,O-η^2 modes. While not a strict necessity, either of these binding modes and particularly the latter would seem to be the most logical for catalyzing the concerted formation of O_2 and Cl^-. By contrast, there are several direct precedents for parts of both mechanisms (2) and (3). The two long-proposed mechanisms for O–O joining in PSII and in synthetic water-splitting catalysts, for example, involve two oxygen atoms poised to react via either nucleophilic or radical processes [1, 2, 112, 113]. Mechanisms that are chemically analogous to pathways (3) and (4) have also been proposed for Fe(III) porphyrin-mediated isomerization of peroxynitrite ($ONOO^-$) to nitrate [114–117]. An Fe(III)-coordinated $ONOO^-$ anion could undergo heterolytic O–N bond cleavage to yield Compound I and the anionic leaving group (nitrite). Nitrite would then act as the nucleophile, attacking Compound I to form nitrate. Alternatively, homolytic O–N bond cleavage would yield Compound II and the neutral, radical leaving group (NO_2). Radical joining of NO_2 and the ferryl oxygen then lead to the Fe(III) porphyrin and NO_3^-.

4.2.3 Catalytic Efficiency

Clds that produce O_2 tend to do so very efficiently. Values for k_{cat}/K_M for several Clds are listed in Table 2, and many are near the diffusion limit. The rapidity with which O_2 is produced has made Clds useful generators of O_2 for stopped flow studies, where oxygen gas is produced within a few milliseconds in an initial mixing experiment between Cld in one syringe and chlorite in another [118]. The oxygenated solution is mixed with a third, concentrated solution of the reduced/anaerobic enzyme species of interest, and the subsequent reaction is monitored. Dioxygen is produced in this way at concentrations of up to 9 mM (25 °C, neutral pH) without observed visible light scattering in a stopped flow reaction chamber, which would be indicative of bubbling. It has been postulated that the solution remains transiently supersaturated over the very short time scale of the initial, O_2-producing mix, although the process of bubble growth has not been explicitly monitored over time.

Having the means to produce very large concentrations of O_2 with rapidity has allowed an important barrier to be surmounted. Namely, many intermediates in reactions between reduced biomolecules and O_2 cannot be observed because they decay more rapidly than they form. However, the second-order rate of their production can be enhanced by increasing $[O_2]$. Using *Da*Cld in this way, that is, as a reagent, has indeed yielded impressive results in cases previously limited by the rapid decay of the intermediate [118]. Other biotechnological applications of the reaction are currently under development.

4.2.4 Reaction Intermediates

While efficiency is critical for a detoxification enzyme and for the experiments described above, it can be the enemy of mechanistic studies. It has thus far not been possible to detect intermediates in the Cld/ClO_2^- reaction (e.g., Compounds 0, I, II) via stopped flow spectrophotometry. Hence, the Cld mechanism has not been monitored directly. By the same token, addition of a variety of colorimetric reagents in the presence of *Da*Cld during turnover with chlorite – small peroxidase substrates such as guaiacol or ascorbate, or the chlorination substrate monochlorodimedone (MCD) – has not resulted in observable side reactivity [105, 119]. This suggests that potential intermediates such as ClO_2 ($\varepsilon_{359\ nm} = 1.23\ mM^{-1}\ cm^{-1}$) [120], ClO^-, or possibly $ClO^{\bullet}$, any of which would react with MCD, either are not generated or cannot be accessed by MCD. The oxidation of molecules like guaiacol or ascorbate by potential intermediates Compound I or II is likewise not observed.

However, *Da*Cld can oxidize the peroxidase substrates guaiacol, ascorbate, and 2,2'-azino-bis(3-ethylbenzothiazoline)-6-sulfonic acid if either peroxide or peracetic acid is the oxidant. Moreover, the transient reactions of *Da*Cld with these oxidants have been examined [89]. These experiments showed that oxygen atom transfer from the peracid donor is very rapid and leads to the formation of Compound I, even in the presence of just one equivalent of oxidant. Hence, while it remains uncertain whether Compound I is an intermediate on the regular reaction pathway with chlorite, it is clear that the enzyme readily forms this species in the presence of another anionic oxygen atom donor that is thermodynamically predisposed toward oxygen atom transfer. These two donors are not identical, however. Unlike chlorite, for which the leaving group is relatively basic and therefore nucleophilic (hypochlorite, $pK_a = 7.5$), peracetic acid leaves behind a much less nucleophilic acetate ion ($pK_a = 4.5$). The reaction between the Fe(III) heme and chlorite would be expected to be catalyzed by a proton donor or positive charge that could stabilize the leaving group. The distal arginine has been proposed to fulfill this role, stabilizing hypochlorite in its anionic form and priming it for re-reaction with the oxygen atom of a hypothetical Compound I.

Interestingly, the *actual* Compound I formed in the reaction between peracetic acid and Fe(III) *Da*Cld reacts avidly with peroxidase substrates [89]. Under stopped flow conditions, a full peroxidase catalytic cycle is observed, with one equivalent of a one-electron donor (ascorbate) forming Compound II and the second returning the intermediate to the Fe(III) form:

$$\mathrm{Fe(III)(porphyrin) + CH_3(C{=}O)COO^- \rightarrow Fe(IV){=}O(porphyrin^{\bullet+}) + CH_3COO^-} \quad (12)$$

$$\mathrm{Fe(IV){=}O(porphyrin^{\bullet+}) + ascorbate \rightarrow Fe(IV){-}OH(porphyrin) + ascorbate^{\bullet}} \quad (13)$$

$$\mathrm{Fe(IV){-}OH(porphyrin) + ascorbate \rightarrow Fe(III)(porphyrin) + ascorbate^{\bullet} + H_2O} \quad (14)$$

These results demonstrate that *Da*Cld's Compound I can access peroxidase-like substrates, which in real peroxidase enzymes are known to bind in different locations above and adjacent to the heme plane [121].

By contrast, H_2O_2 reacts much more slowly with Fe(III) *Da*Cld than peracetic acid and, rather than producing Compound I, the only observed spectroscopic changes following the reaction correspond to heme oxidation. This observation is consistent with the Clds' lack of a distal pocket base. A distal histidine is absolutely required for rapid Compound I formation in the well-studied plant peroxidases [122–125]. When this residue is mutated to an aliphatic amino acid, the rate of Compound I formation slows by five orders of magnitude. In short, *Da*Cld can be a very effective peroxidase, but only in the presence of an acidic oxygen atom donor to the Fe(III) heme, for which a distal base is not required.

The *Da*Cld Compound I intermediate is not long-lived. It spontaneously converts to a ferryl without a coupled porphyrin cation radical. This conversion becomes more rapid at higher pH. The relative instability of Compound I is consistent with the generation of O_2 from a single molecule of chlorite. Namely, if Compound I is an intermediate on the O_2 production pathway, it may be too short-lived to react with oxygen-atom donors that are not already in the vicinity of the ferryl. Indeed, a Compound I species prepared in the stopped flow did not react with exogenously supplied ClO^-/HClO to form O_2, as the reaction appears to be kinetically out-competed by decay of the Compound I intermediate [89]. Though the pathway has not been studied, Compound I's breakdown has been presumed to occur via the conserved tyrosines that ring (and in one case form hydrogen bonds with) the heme [79].

Finally, although oxidation of guaiacol/ascorbate or chlorination of MCD is not observed during *Da*Cld/chlorite turnover, the peroxidase substrates increase (~10-fold) the number of molecules of chlorite that *Da*Cld can decompose before it irreversibly inactivates. The high valent intermediates are returned to the Fe(III) state and hence to activity with chlorite by these substrates. A similar type of "rescue" is likewise observed in other heme proteins [126–128]. This suggests that Compounds I, II, or both are intermediates on the pathway to whatever limits the catalytic lifetime of Clds (see below.) By contrast, MCD has no such rescuing effect, suggesting either that diffusible O/Cl species are not produced or are not appreciably responsible for substrate-dependent inactivation of *Da*Cld.

4.2.5 Structure-Activity Relationships: Highlights

The active site of the typical *bona fide,* chlorite-degrading Cld was discussed above in terms of what it is; it is also worthwhile to consider what it *is not*. Unlike peroxidases, which characteristically have a histidine-arginine pair in their distal pockets, Clds possess an arginine as the sole conserved, polar residue. The distal histidine is critical for peroxidase function as described above, acting as a base to deprotonate H_2O_2 and then as an acid toward the resulting Fe(III)-OOH (Compound 0) intermediate to generate Compound I and water. Such proton

motions are critical for the rapid formation of both Compound 0 and Compound I in other heme proteins that activate O_2 or H_2O_2. Fe(III) Clds lack both a distal basic residue and a recognizable proton conduit to the heme iron. Perhaps not surprisingly, Clds bind anionic CN^- and $CH_3(C{=}O)COO^-$ (surrogates for OOH^-) much faster than protonated HCN or H_2O_2 [104]. *Da*Cld also rapidly forms Compound I following reaction with peracetic acid but not H_2O_2 [89]. In short, Clds lack the necessary machinery for efficiently binding and activating peroxide, and this colors what they can and cannot efficiently do with biological oxidants.

By contrast, Clds readily bind anions, including the substrate chlorite. Here, the distal arginine plays a key role. In multiple crystal structures, it forms a hydrogen bond to the axial ligand bound to the Fe(III) iron, from which it is separated by ~3 Å [4, 76, 80, 82]. Notably, the arginine has no identifiable hydrogen bonding partners among either the active site amino acids or the heme propionates, though an Arg-propionate interaction is present in some DyPs [83]. *Da*Cld, in fact, does not crystalize in the absence of a heme ligand, possibly in part because the motion of this residue would otherwise remain unrestrained. Resonance Raman experiments support a model where the arginine side chain interacts with axially-bound distal ligands and assumes different orientations ("in" or "out," relative to the heme plane) as a function of pH [78, 98]. In solution, substitution of the arginine with neutral glutamine by mutagenesis results in a strongly diminished k_{cat}/K_M(chlorite) and in a loss of affinity for anions [78]. This indicates that arginine is indeed critical for stabilizing the Michaelis complex, presumed to be a Compound 0-like Fe(III)-chlorito species [78].

The distal arginine is also sufficient for promoting rapid, heterolytic cleavage of the peracid O–O bond and stabilizing the resulting Compound I intermediate [89]. Similar functions have been attributed to the distal arginine in classical peroxidases, though in conjunction with an anionic proximal ligand to the heme iron. In peroxidases, anionic or histidinate character in this ligand is understood to add electron density to the Fe(III) and to consequently support heterolytic cleavage of a bond coordinated in *trans*. As described by the classic "push-pull" model of peroxidase catalysis, the electron-rich proximal ligand supplies a "push" toward cleaving a coordinated O–O bond, while the distal arginine supplies a concurrent "pull" [96, 124, 129]. The imidazole ring of the histidine gains anionic character via hydrogen bonding to an aspartate or glutamate. Though *Da*Cld has such a His-Glu hydrogen bond, resonance Raman showed the proximal ligand to be neutral in character [98]. O–O bond cleavage is relatively rapid in *Da*Cld in spite of the nature of the protein-derived ligand on the proximal side of the heme iron, suggesting that the distal pocket's "pull" alone is enough. The fact that *Da*Cld readily cleaves the O–O bond of coordinated peracetate ion also suggests that, in principle, it should be able to heterolytically cleave the O–Cl bond of a bound chlorite with similar avidity.

The mobility of the arginine could be important for an additional, important function: stabilizing the hypochlorite/hypochlorous acid (aqueous $pK_a = 7.5$) formed when the O–Cl bond of chlorite is broken. Nucleophilic attack of the leaving group on Compound I should be significantly more avid for the

deprotonated hypochlorite than for hypochlorous acid, as described above. The positive charge of the arginine could locally lower the pK_a for the anion/acid pair, stabilizing the hypochlorite. It could also steer the hypochlorite into an optimal position for nucleophilic attack on Compound I.

Finally, the distal arginine could not manage to be such a key player were it not for a supporting cast of conserved, hydrophobic residues surrounding it. These residues constitute a sterically confined, chemically unreactive low ceiling over the heme plane [4]. Such an enclosed environment seems ideal for enforcing the recombination of a hypochlorite leaving group with Compound I.

4.2.6 Heme and Protein Stability in Diverse Chlorite Dismutase Family Proteins

The pentameric O_2-evolving *Da*Cld catalyzes ~20,000 turnovers (per heme) before irreversibly inactivating. The same number of chlorite equivalents completely eliminates the heme chromophore [105]. This suggests that oxidative destruction of the heme is responsible for the observed irreversible inactivation. Indeed, heme scission is a common side effect of oxidative catalysis: playing with matches will eventually cause even a robustly designed protein to get burned.

The mechanism of heme decomposition has not been studied. It has been observed, however, that far fewer turnovers are sustained by structurally distinct Clds [76]. The dimeric Cld from *Klebsiella pneumoniae*, for example, contains a distal arginine and catalyzes the chlorite to O_2 conversion with steady state parameters similar to those measured for *Da*Cld. However, the lifetime of the enzyme is clearly shorter; the measured turnover number is only 2,000–3,000 per heme [104]. The pentameric Cld from *Staphylococcus aureus* has a glutamine in place of the distal arginine. Its heme disappears following incubation with fewer than five equivalents of chlorite, and no O_2 evolution from this protein is observed [75]. The structural features leading to the great disparity in heme stability across the Cld family are not understood.

5 Synthetic and Biochemical Models

5.1 Chlorite as Reagent with Related Synthetic Metalloporphyrins

Quite apart from Clds and O_2 generation, NaOCl and $NaClO_2$ have an illustrious history as reagents in metalloporphyrin chemistry. Like iodosylbenzene, organic peracids (RCO_3H), and $KHSO_5$, the oxochlorates have been used as so-called "shunt" reagents: oxygen atom donors that, unlike O_2, do not require the input of a pair of activating electrons from the catalyst. Such shunt reagents have been used

extensively in studies of cytochrome P450 monooxygenases and their synthetic mimics [130–132]. They have also been used in studies of peroxidases and heme oxygenases, where the oxygen-atom transfers to a Fe(III) heme center to yield Compound I. The same intermediate can equivalently be reached by the addition of O_2, three electrons, and one proton to a Fe(II) heme (P450), or peroxide minus one proton to the Fe(III) heme (peroxidases), with water as the leaving group.

Motivated by the goals of understanding and possibly mimicking P450 chemistry, Collman et al. were the first to describe O_2 evolution from synthetic Mn(III)porphyrin catalysts and ClO_2^- in non-aqueous media [133]. O_2 production occurred as a side reaction to a more P450-like process: the oxidation of unactivated alkanes (e.g., cyclohexane), which were converted in a two-electron process to alcohols and in a four-electron process to ketones. Notably, the turnover numbers using chlorite were >40-fold higher than if other oxygen-atom donors were used, and the ketone/alcohol ratio was at least double. These results suggested that chlorite was acting as something other than a simple oxygen-atom donor to the manganese. Further investigation then showed that radical trapping agents inhibited turnover, indicating that the Mn(III)/chlorite system acted as a radical initiator.

A two-pathway scheme was proposed to explain the observed oxidations of cyclohexane to cyclohexanol and cyclohexanone (Figure 11) [132]. In the first pathway, a Mn(III)/chlorite-derived species was proposed to generate a cyclohexyl radical by hydrogen-atom ($H^\bullet$) abstraction. The organic radical then combined with O_2 to form a peroxyl radical adduct. The reaction of two such C_6H_{11}-$OO^\bullet$ species would then lead to the formation of cyclohexanol, cyclohexanone, and, notably, O_2. A radical process helped explain the observation of ketone products, which were shown not to arise from the oxidation of alcohols formed initially as precursors. In the second proposed pathway, oxygen atom transfer from chlorite to the manganese(III)porphyrin catalyst (via heterolytic Cl–O bond cleavage) was proposed to yield a formal Mn(V)=O species and ClO^- as the leaving group. The high valent Mn(V)=O could then react via a more conventional, P450-like rebound mechanism to form the hydroxylation product:

$$\mathrm{Mn(V){=}O + C_6H_6 \rightarrow Mn(IV){-}OH + C_6H_5^\bullet \rightarrow C_6H_5{-}OH + Mn(III)} \qquad (15)$$

In addition to the two alkane-oxidizing pathways, simple, metal-catalyzed decomposition of chlorite by two routes was also observed. In the first, Cl^- and O_2 were produced. Though a mechanism was not explicitly offered, it is possible that Mn(V)=O and Cl^- combined in the same manner proposed for the enzymatic/Cld reaction. The second pathway led to conversion of chlorite to chlorate and chloride in a 3:2:1 ratio:

$$3\ ClO_2^- \rightarrow 2\ ClO_3^- + Cl^- \qquad (16)$$

Because the manganese catalysts are inert toward chlorate, it persisted here as a dead-end product.

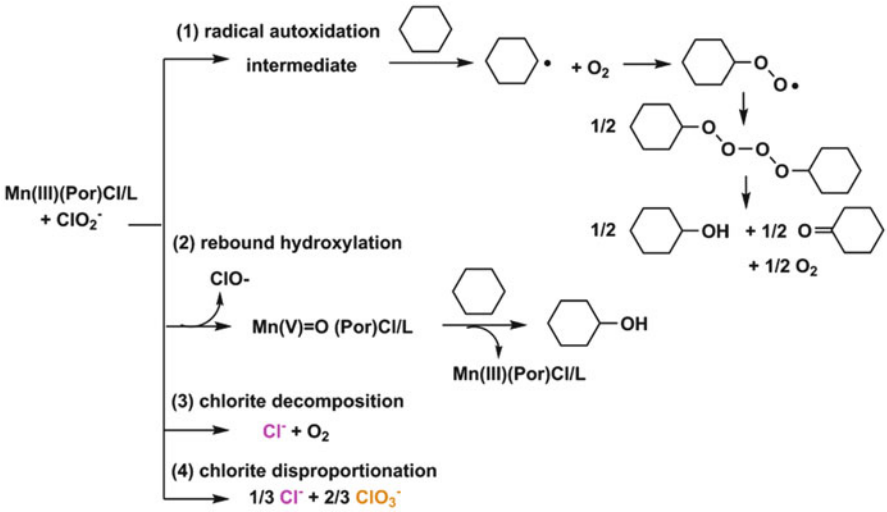

Figure 11 Reactions of Mn(III)porphyrin complexes (Por = porphyrin and L = *t*-butyl-pyridine) with chlorite and cyclohexane, where the use of chlorite as a P450-like "shunt" oxidant was tested. In pathway (1), an unknown Mn/chlorite intermediate forms a cyclohexyl radical. This reacts with O_2, either from air or produced from chlorite via pathway (3). Coupling of two peroxyl radicals ultimately leads to equimolar cyclohexanone, cyclohexanol, and O_2. Pathway (2) begins with the formation of a Mn(V)=O species via oxygen atom transfer from chlorite. This intermediate extracts a hydrogen atom from cyclohexane, forming the cyclohexyl radical and Mn(IV)–OH. Mn(IV)–OH and the radical recombine to yield the Mn(III)(Por)Cl starting material and cyclohexanol product. Finally, pathway (3) illustrates direct decomposition of chlorite to yield chloride and dioxygen, and pathway (4) shows its disproportionation. Scheme adapted from [133].

The laboratory of Abu-Omar subsequently investigated O_2 generation from metalloporphyrin/chlorite systems as the target reaction rather than as a side process [134–136]. Water-soluble iron porphyrin complexes with different aryl groups at the four *meso* positions were studied (Figure 12) as models for Clds. The *p*-sulfonatophenyl- and *N*,*N*,*N*-trimethylanilinium-substituted Fe(III) porphyrins led primarily to the same kind of chlorite-to-chlorate disproportionation observed by Collman et al. (eqn. 16) [133]. This mechanism of the reaction was studied in some detail, and shown to occur via the initial formation of an Fe(IV)=O(porphyrin$^{\bullet+}$) (Compound I) intermediate. Compound I was proposed to comproportionate with an aqua-Fe(III)porphyrin, resulting in a pair of Fe(IV)–OH(porphyrin) (Compound II) species. Compound II would then transfer its oxygen atom to chlorite, generating chlorate and the two-electron reduction product of the catalyst, Fe(II)porphyrin. The Fe(II)porphyrin thus formed can react with both chlorite and hypochlorite, heterolytically cleaving their Cl–O bonds and generating further reactive Fe(IV)–OH(porphyrin).

Though the first two iron porphyrins did not produce O_2 from chlorite, the fluorinated analog of one of them, [Fe(III)(TF_4TMAP)](OTf)$_5$, did in 18 % yield

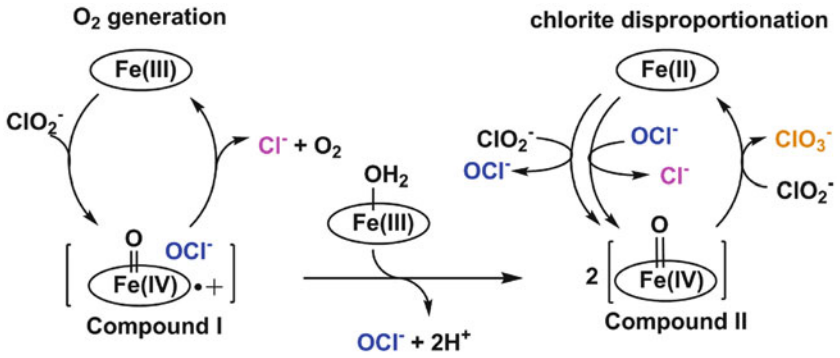

Figure 12 Reactions of $[Fe(III)TF_4TMAP]^{5+}$, yielding O_2, Cl^-, ClO_3^- as ultimate end products. The O_2-generating mechanism on the left resembles the heterolytic/nucleophilic pathway proposed for Clds in Figure 11. The Compound I-like intermediate can react with another molecule of the aquated, Fe(III) catalyst, yielding two equivalents of Compound II (ferryl). This intermediate reacts with further equivalents of chlorite to produce chlorate and the Fe(II) catalyst. Adapted from [135].

[OTf = triflate, TF_4TMAP = 5,10,15,20-tetrakis(tetrafluro-*N,N,N*-trimethylanilinium) porphyrinato]. The remaining chlorite followed the more customary pathway of disproportionation to chlorate and chloride. Production of O_2 was proposed to begin with oxygen atom transfer from chlorite to the Fe(III)porphyrin, forming Compound I. The same step was invoked as in the initiating step for chlorate generation. However, circa 1/5 of the time, the Compound I intermediate reacts with ClO^- instead of another Fe(III)porphyrin, generating O_2 and Cl^-. Notably, enclosure of the ClO^- leaving group and Fe(IV)=O(porphyrin$^{+\bullet}$) species, as well as site-isolation of the reactive metal, would both in principle improve the O_2 yield from the otherwise catalytically competent Fe(III)porphyrin. Isolation of the reactive intermediates is an obvious role served by the Cld protein environment.

In addition to the disporoportionation and O_2 generation reactions described above, some manganese(III)porphyrins catalyze yet a further transformation of chlorite: its one electron oxidation to the chlorine dioxide (ClO_2) radical (Figure 13) [137, 138]. This reaction is preferentially catalyzed by the water-soluble Mn(III) analogs of $[Fe(III)(TF_4TMAP)]^{5+}$ and by tetrakis-5,10,15,20-(N,N-dimethylimidazolium) porphyrinatomanganese(III), $[Mn(TDMImP)]^{5+}$. In each case, the reaction was proposed to begin with oxygen atom transfer to the Mn(III), generating the Mn(V)=O product of heterolytic Cl–O bond cleavage in the $[Mn(TDMImP)]^{5+}$ system and a mixture of the heterolytic and homolytic (Mn(IV)=O) products in the presence of $[Mn(TF_4TMAP)]^{5+}$. The ClO^- leaving group was able to re-enter the catalytic cycle as an oxygen-atom donor to Mn(III) porphyrin. The $ClO^\bullet$ (product of homolytic Cl–O cleavage) was proposed to react in an uncatalyzed fashion with additional molecules of ClO_2^-. The high-valent metal-oxo species produced in either case served as one-electron oxidants toward chlorite [109], generating neutral chlorine dioxide gas (eqn. 11).

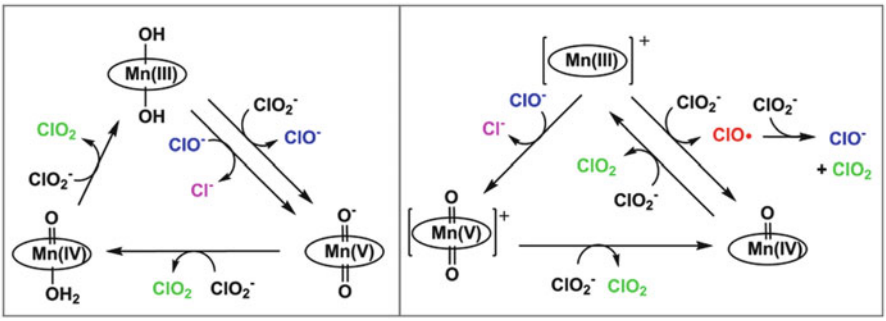

Figure 13 Reactions of Mn(III)porphyrins with chlorite to produce ClO_2. **Left**: Oxygen-atom transfer from chlorite yields a Mn(V)=O species that is then capable of two, sequential one-electron oxidations of a pair of chlorite anions in a peroxidase-like catalytic cycle (products = $2ClO_2$, green; manganese ligand = TDMImP). **Right**: A slightly more complicated proposed mechanism begins with electron transfer followed by atom transfer to the Mn(III)porphyrin (L = TF_4TMAP), forming an Mn(IV)=O species and $ClO^{\bullet}$. The latter reacts with chlorite to form ClO_2 and ClO^-. Hypochlorite reacts with Mn(III)porphyrin to form a Mn(V)-dioxo species analogous to that in the left-hand panel, which oxidizes two molecules of chlorite to yield two ClO_2. Figure adapted from [137] and [138].

This reaction is interesting in itself from a technological point of view, because ClO_2 is a reagent used in water purification that must be produced near its point of use because it cannot be easily compressed and stored. It also provides a potential mechanistic contrast with Clds and the porphyrin complexes which generate Compound I but appear to use it to transfer an oxygen atom to hypochlorite (a two-electron process) rather than for the one-electron oxidation of chlorite. Presumably, recombination between the Compound I and hypochlorite generated in the confined space above the Cld heme kinetically out-competes the reaction between Compound I and another molecule of chlorite. This is a hypothesis that awaits further experimental investigation.

5.2 *Reactions of Chlorite with Horseradish Peroxidase: Implications for Chlorite Dismutases*

The use of chlorite as both an oxidant (oxygen-atom donor) and one-electron reductant by the Mn(III)porphyrins mirrors the results of a careful, systematic study of the reactions of horseradish peroxidase (HRP) and chlorite [120]. The complexity of this reaction had been previously noted [139, 140]. In strong contrast to Clds, Fe(III) HRP reacted with both chlorite and hypochlorite as oxygen-atom donors (generating Compound I), followed by two molecules of chlorite serving as one-electron donors to return the intermediate to the Fe(III) state (i.e., a complete peroxidase-like catalytic cycle, eqs 12–14). The chlorine dioxide products were also capable of donating an oxygen atom to the Fe(III) HRP, yielding Compound I and chlorine oxide (Figure 14). The ultimate fate of the highly-reactive $ClO^{\bullet}$ radical was not clear.

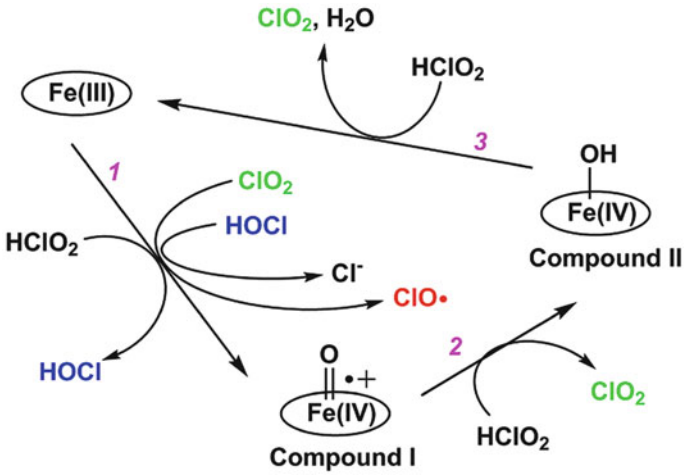

Figure 14 Reactions of horseradish peroxidase with chlorite. In the first step of the reaction (1), charge-neutral chlorous acid transfers an oxygen atom to Fe(III) HRP to form Compound I and hypochlorite/hypochlorous acid. Compound I then catalyzes two sequential one-electron oxidations of chlorous acid molecules (steps 2 and 3), producing two molecules of chlorine dioxide and returning the heme to the Fe(III) state. The inside of the diagram shows how both HClO and ClO_2 are able to re-enter the catalytic cycle as oxygen atom donors, producing Compound I and either Cl^- or $ClO^\bullet$ as the leaving groups, respectively. Figure adapted from [120].

In spite of having a relatively well-enclosed active site that could in principle contain and steer $ClO^-/ClO^\bullet$ leaving groups, neither appeared to recombine with the HRP-ferryl to make O_2. The reasons for this are unknown; however, the pH dependence of the HRP reactions with chlorite may lend clues. Compound I formation from Fe(III) HRP and ClO^- or ClO_2^-, but not ClO_2, was highly dependent on pH. In keeping with HRP's known preference for neutral ligands, including peroxide [141], the neutral/protonated species (HClO, $HClO_2$) reacted preferentially with the Fe(III) iron. The distal histidine in HRP and all the well-studied plant peroxidases is critical for H_2O_2 deprotonation to form the Fe(III)-OOH (Compound 0) complex. It may similarly be involved in deprotonating chlorous acid ($HClO_2$, $pK_a = 1.72$) [20, 123]. By contrast, Clds lack a distal histidine and strongly prefer to bind cyanide and peracids in their anionic forms, with the distal arginine helping to secure the bound anion [78, 89]. The subsequent reactions of HRP-Compounds I and II with chlorite were also highly pH-dependent. The plotted dependencies of log *k versus* pH were once again linear with a slope of −1, indicating that Compounds I and II preferentially react with the $HClO_2$ acid rather than ClO_2^-, in spite of the relative scarcity of the acid form (pK_a 1.72) in biochemically obtainable pH ranges. Again in contrast, it has been proposed that Compound I in Clds reacts with hypochlorite in its anionic form, in part because ClO^- is a better nucleophile than the HClO acid (pK_a 7.5), and in part because the steady state reaction is faster at low pH, where the distal arginine is expected to point toward the heme plane and to stabilize the ClO^- leaving group [78, 98]. The Clds' ability to stabilize the hypochlorite leaving group in its anionic form may be critical for

promoting O–O bond formation, and for distinguishing Clds from (O)Cl–O^- bond-cleaving, Compound I-forming peroxidases that nonetheless do not make O_2, such as HRP.

Alternatively or in addition, peroxidases are conventionally understood to react with their substrates on the periphery of the heme rather than at the apex of the distal pocket [121, 142–144]. Direct reaction of the porphyrin cation radical and substrate prevents cytochrome-P450-like oxygen-atom transfer from the Compound I intermediate to the substrate, which occurs when the substrate is able to approach the ferryl oxygen from an optimal angle. In Clds, reaction of hypochlorite with Compound I requires access to the same ferryl oxygen atom, while peroxidase-style one-electron reductions can just as well occur at the heme edge. It is possible that, in HRP, the distal pocket is not sterically configured to promote attack of the ClO^-/HClO leaving group on the ferryl oxygen. Hence, O_2 production is not observed.

6 General Conclusions

As work with Clds illustrates, there is seemingly nothing that nature can't do with a protein and a heme. The unusual transformation of ClO_2^- to O_2 and Cl^- is greatly facilitated by enclosing heme in the relatively hydrophobic environment of chlorite dismutase, with a well-positioned arginine needed to recruit and steer the anionic substrate and intermediates. The arginine is a key innovation in an active site pocket that seems otherwise well-suited for little more than heme decomposition. The etiology of chlorite decomposition by Clds, the history of this fascinating protein family, and the biogeochemical consequences of natural perchlorate respiration all remain to be discovered by ongoing and future work.

Abbreviations and Definitions

Cld	chlorite dismutase
ClO^-	hypochlorite
ClO_2	chlorine dioxide
ClO_2^-	chlorite
ClO_3^-	chlorate
ClO_4^-	perchlorate
Clr	chlorate reductase
Compound 0	Fe(III)-anion complex
Compound I	Fe(IV)porphyrin cation radical
Compound II	Fe(IV)=O or Fe(IV)–OH
*Da*Cld	*Dechloromonas aromatica* chlorite dismutase
DMSO	dimethylsulfoxide

DyP	dye-decoloring peroxidase
HClO	hypochlorous acid
HRP	horseradish peroxidase
MCD	monochlorodimedone
MGD	molybdopterin guanine dinucleotide
Nar	nitrate reductase
NHE	normal hydrogen electrode
NPRB	non-perchlorate-respiring bacteria
*Nw*Cld	*Nitrospira winogradskyi* chlorite dismutase
$ONOO^-$	peroxynitrite
OTf	triflate
Pcr	perchlorate reductase
(per)chlorate	chlorate and/or perchlorate
PRB	perchlorate-respiring bacteria
PSII	Photosystem II
Ser	selenate reductase
TDMImP	tetrakis-5,10,15,20-(N,N-dimethylimidazolium)porphyrinato
TF_4TMAP	5,10,15,20-tetrakis(tetrafluro-*N*,*N*,*N*-trimethylanilinium) porphyrinato
WCL	wet chemistry laboratory

Acknowledgments Support for this work from the National Institutes of Health, National Institute for General Medical Sciences is gratefully acknowledged (GM090260), as are the scientific and intellectual contributions of laboratory members past and present.

References

1. C. S. Mullins, V. L. Pecoraro, *Coord. Chem. Rev.* **2008**, *252*, 416–443.
2. J. P. McEvoy, G. W. Brudvig, *Chem. Rev.* **2006**, *106*, 4455–4483.
3. K. N. Ferreira, T. M. Iverson, K. Maghlaoui, J. Barber, S. Iwata, *Science* **2004**, *303*, 1831–1838.
4. B. R. Goblirsch, B. R. Streit, J. L. DuBois, C. M. Wilmot, *J. Biol. Inorg. Chem.* **2010**, *15*, 879–888.
5. K. A. Weber, L. A. Achenbach, J. D. Coates, *Nature Rev. Microbiol.* **2006**, *4*, 752–764.
6. J. D. Coates, U. Michaelidou, R. A. Bruce, S. M. O'Connor, J. N. Crespi, L. A. Achenbach, *Appl. Environ. Microbiol.* **1999**, *65*, 5234–5241.
7. K. Kim, B. E. Logan, *Water Res.* **2001**, *35*, 3071–3076.
8. B. E. Logan, J. Wu, R. F. Unz, *Water Res.* **2001**, *35*, 3034–3038.
9. B. E. Logan, H. S. Zhang, P. Mulvaney, M. G. Milner, I. M. Head, R. F. Unz, *Appl. Environ. Microbiol.* **2001**, *67*, 2499–2506.
10. H. S. Zhang, M. A. Bruns, B. E. Logan, *Environ. Microbiol.* **2002**, *4*, 570–576.
11. R. A. Bruce, L. A. Achenbach, J. D. Coates, *Environ. Microbiol.* **1999**, *1*, 319–329.
12. C. W. Trumpolt, M. Crain, G. D. Cullison, S. J. P. Flanagan, L. Siegel, S. Lathrop, *Remediation* **2005**, *Winter*, 65–89.

13. R. Renner, *Environ. Sci. & Tech. News* **1998**, *32*, 210A.
14. E. T. Urbansky, *Bioremediation J.* **1998**, *2*, 81–95.
15. E. T. Urbansky, S. K. Brown, *J. Environ. Monitor.* **2003**, *5*, 455–462.
16. E. T. Urbansky, M. R. Schock, *J. Environ. Manage.***1999**, *56*, 79–95.
17. J. S. Valentine, C. S. Foote, A. Greenberg, J. F. Liebman, *Active Oxygen in Biochemistry*, Eds J. S. Valentine, C. S. Foote, A. Greenberg, J. F. Lieberman, Springer, Dordrecht, **1995**, pp. 481.
18. I. R. Epstein, K. Kustin, *J. Phys. Chem.* **1985**, *89*, 2275–2282.
19. J. Arnhold, E. Monzani, P. G. Fürtmuller, M. Zederbauer, L. Casella, C. Obinger, *Eur. J. Inorg. Chem.* **2006**, 3801–3811.
20. I. Fabian, G. Gordon, *Inorg. Chem.* **1991**, *30*, 3785–3787.
21. E. T. Urbansky, *Environ. Sci. Pollut. Res.* **2002**, *9*, 187–192.
22. P. K. DasGupta, J. V. Dyke, A. B. Kirk, W. A. Jackson, *Environ. Sci. Tech.* **2006**, *40*, 6608–6614.
23. E. T. Urbansky, *Environmental Impact of Fertilizer on Soil and Water* **2004**, *872*, 16–31.
24. E. T. Urbansky, S. K. Brown, M. L. Magnuson, C. A. Kelty, *Environ. Pollut.* **2001**, *112*, 299–302.
25. G. E. Ericksen, *Amer. Sci.* **1983**, *71*, 366–374.
26. H. M. Bao, B. H. Gu, *Environ. Sci. Tech.* **2004**, *38*, 5073–5077.
27. B. R. Scanlon, R. C. Reedy, W. A. Jackson, B. Rao, *Environ. Sci. Tech.* **2008**, *42*, 8648–8653.
28. B. Rao, T. A. Anderson, G. J. Orris, K. A. Rainwater, S. Rajagopalan, R. M. Sandvig, B. R. Scanlon, D. A. Stonestrom, M. A. Walvoord, W. A. Jackson, *Environ. Sci. Tech.* **2007**, *41*, 4522–4528.
29. S. Rajagopalan, T. A. Anderson, L. Fahlquist, K. A. Rainwater, M. Ridley, W. A. Jackson, *Environ. Sci. Tech.* **2006**, *40*, 3156–3162.
30. S. P. Kounaves, S. T. Stroble, R. M. Anderson, Q. Moore, D. C. Catling, S. Douglas, C. P. McKay, D. W. Ming, P. H. Smith, L. K. Tamppari, A. P. Zent, *Environ. Sci. Tech.* **2010**, *44*, 2360–2364.
31. D. K. Tipton, D. E. Rolston, K. M. Scow, *J. Environ. Quality* **2003**, *32*, 40–46.
32. L. N. Plummer, J. K. Bohlke, M. W. Doughten, *Environ. Sci. Tech.* **2006**, *40*, 1757–1763.
33. B. A. Rao, C. P. Wake, T. Anderson, W. A. Jackson, *Water, Air, Soil Pollut.* **2012**, *223*, 181–188.
34. V. I. Furdui, F. Tomassini, *Environ. Sci. Tech.* **2010**, *44*, 588–592.
35. G. Bordeleau, R. Martel, G. Ampleman, S. Thiboutot, *J. Environ. Qual.* **2008**, *37*, 308–317.
36. N. C. Sturchio, J. R. Hoaglund, III, R. J. Marroquin, A. D. Beloso, Jr., L. J. Heraty, S. E. Bortz, T. L. Patterson, *Ground Water* **2012**, *50*, 94–102.
37. P. N. Smith, C. W. Theodorakis, T. A. Anderson, R. J. Kendall, *Ecotoxicology* **2001**, *10*, 305–313.
38. M. L. Magnuson, E. T. Urbansky, C. A. Kelty, *Analyt. Chem.* **2000**, *72*, 25–29.
39. P. K. Dasgupta, A. B. Kirk, J. V. Dyke, S.-I. Ohira, *Environ. Sci. Tech.* **2008**, *42*, 8115–8121.
40. J. V. Dyke, K. Ito, T. Obitsu, Y. Hisamatsu, P. K. Dasgupta, B. C. Blount, *Environ. Sci. Tech.* **2007**, *41*, 88–92.
41. A. B. Kirk, M. Kroll, J. V. Dyke, S.-I. Ohira, R. A. Dias, P. K. Dasgupta, *Sci. Tot. Environ.* **2012**, *420*, 73–78.
42. W. Wallace, T. Ward, A. Breen, H. Attaway, *J. Indust. Microbiol.* **1996**, *16*, 68–72.
43. G. Rikken, A. Kroon, C. van Ginkel, *Appl. Microbiol. Biotech.* **1996**, *45*, 420–426.
44. P. K. Dasgupta, P. K. Martinelango, W. A. Jackson, T. A. Anderson, K. Tian, R. W. Tock, S. Rajagopalan, *Environ. Sci. Tech.* **2005**, *39*, 1569–1575.
45. B. Rao, S. Mohan, A. Neuber, W. A. Jackson, *Water, Air, Soil Pollut.* **2012**, *223*, 275–287.
46. L. Jaegle, Y. L. Yung, G. C. Toon, B. Sen, J. F. Blavier, *Geophys. Res. Lett.* **1996**, *23*, 1749–1752.
47. R. Simonaitis, J. Heicklen, *Planet. Space Sci.* **1975**, *23*, 1567–1569.
48. M. H. Hecht, S. P. Kounaves, R. C. Quinn, S. J. West, S. M. M. Young, D. W. Ming, D. C. Catling, B. C. Clark, W. V. Boynton, J. Hoffman, L. P. DeFlores, K. Gospodinova, J. Kapit, P. H. Smith, *Science* **2009**, *325*, 64–67.

49. J. D. Schuttlefield, J. B. Sambur, M. Gelwicks, C. M. Eggleston, B. A. Parkinson, *J. Am. Chem. Soc.* **2011**, *133*, 17521–17523.
50. K. S. Bender, C. Shang, R. Chakraborty, S. M. Belchik, J. D. Coates, L. A. Achenbach, *J. Bacteriol.* **2005**, *187*, 5090–5096.
51. J. C. Thrash, J. Pollock, T. Torok, J. D. Coates, *Appl. Microbiol. Biotech.* **2010**, *86*, 335–343.
52. J. C. Thrash, S. Ahmadi, T. Torok, J. D. Coates, *Appl. Microbiol. Biotech.* **2010**, *76*, 4730–4737.
53. C. I. Carlstrom, O. Wang, R. A. Melnyk, S. Bauer, J. Lee, A. Engelbrektson, J. D. Coates, *MBio* **2013**, *4*, 00217–13.
54. M. Balk, T. van Gelder, S. A. Weelink, A. J. A. Stams, *Appl. Environ. Microbiol.* **2008**, *74*, 403–409.
55. M. Balk, F. Mehboob, A. H. van Gelder, W. I. C. Rijpstra, J. S. S. Damste, A. J. M. Stams, *Appl. Microbiol. Biotech.* **2010**, *88*, 595–603.
56. C. P. Shelor, A. B. Kirk, P. K. Dasgupta, M. Kroll, C. A. Campbell, P. K. Choudhary, *Environ. Sci. Tech.* **2012**, *46*, 5151–5159.
57. M. G. Liebensteiner, M. W. H. Pinkse, P. J. Schaap, A. J. M. Stams, B. P. Lomans, *Science* **2013**, *340*, 85–87.
58. H. D. Thorell, K. Stenklo, J. Karlsson, T. Nilsson, *Appl. Environ. Microbiol.* **2003**, *69*, 5585–5592.
59. A. Wolterink, A. B. Jonker, S. W. M. Kengen, A. J. M. Stams, *Int. J. Syst. Evol. Microbiol.* **2002**, *52*, 2183–2190.
60. K. Yoshimatsu, T. Sakurai, T. Fujiwara, *FEBS Lett.* **2000**, *470*, 216–220.
61. R. M. Martinez-Espinosa, E. J. Dridge, M. J. Bonete, J. N. Butt, C. S. Butler, F. Sargent, D. J. Richardson, *FEMS Microbiol.* **2007**, *276*, 129–139.
62. A. McEwan, J. Ridge, C. McDevitt, P. Hugenholtz, *Geomicrobiol. J.* **2002**, *19*, 3–21.
63. J. D. Coates, R. Chakraborty, J. G. Lack, S. M. O'Connor, K. A. Cole, K. S. Bender, L. A. Achenbach, *Nature* **2001**, *411*, 1039–1043.
64. K. G. Byrne-Bailey, J. D. Coates, *J. Biotech.* **2012**, *194*, 2767–2768.
65. R. A. Melnyk, A. Engelbrektson, I. C. Clark, H. K. Carlson, K. Byrne-Bailey, J. D. Coates, *Appl. Environ. Microbiol.* **2011**, *77*, 7401–7404.
66. I. C. Clark, R. A. Melnyk, A. Engelbrektson, J. D. Coates, *mBio* **2013**, *4*, 00379–13.
67. S. Weelink, N. Tan, H. ten Broeke, C. van den Kieboom, W. van Doesburg, A. Langenhoff, J. Gerritse, H. Junca, A. Stams, *Appl. Environ. Microbiol.* **2008**, *74*, 6672–6681.
68. M. Oosterkamp, T. Veuskens, C. Plugge, A. Langenhoff, J. Gerritse, W. van Berkel, D. Pieper, H. Junca, L. Goodwin, H. Daligault, D. Bruce, J. Detter, R. Tapia, C. Han, M. Land, L. Hauser, H. Smidt, A. Stams, *J. Bacteriol.* **2011**, *193*, 5028–5029.
69. J. D. Coates, L. A. Achenbach, *Nature Rev. Microbiol.* **2004**, *2*, 569–580.
70. T. Nilsson, M. Rova, A. S. Backlund, *Biochim. Biophys. Acta* **2013**, *1827*, 189–197.
71. F. Maixner, M. Wagner, S. Lucker, E. Pelletier, S. Schmitz-Esser, K. Hace, E. Spieck, R. Konrat, D. Le Paslier, H. Daims, *Environ. Microbiol.* **2008**, *10*, 3043–3056.
72. K. S. Bender, M. R. Rice, W. H. Fugate, J. D. Coates, L. A. Achenbach, *Appl. Environ. Microbiol.* **2004**, *70*, 5651–5658.
73. A. S. Backlund, J. Bohlin, N. Gustavsson, T. Nilsson, *Appl. Environ. Microbiol.* **2009**, *75*, 2439–2445.
74. A. Ebihara, A. Okamoto, Y. Kousumi, H. Yamamoto, R. Masui, N. Ueyama, S. Yokoyama, S. Kuramitsu, *J. Struct. Funct. Gen.* **2005**, *6*, 21–32.
75. J. A. Mayfield, N. D. Hammer, R. C. Kurker, T. K. Chen, S. Ojha, E. P. Skaar, J. L. DuBois, *J. Biol. Chem.* **2013**, *288*, 23488–23504.
76. G. Mlynek, B. Sjoeblom, J. Kostan, S. Fuereder, F. Maixner, K. Gysel, P. G. Fürtmueller, C. Obinger, M. Wagner, H. Daims, K. Djinovic-Carugo, *J. Bacteriol.* **2011**, *193*, 2408–2417.
77. K. S. Bender, S. A. O'Connor, R. Chakraborty, J. D. Coates, L. A. Achenbach, *Appl. Environ. Microbiol.* **2002**, *68*, 4820–4826.

78. B. Blanc, J. A. Mayfield, C. A. McDonald, G. S. Lukat-Rodgers, K. R. Rodgers, J. L. DuBois, *Biochemistry* **2012**, *51*, 1895–1910.
79. B. Blanc, K. R. Rodgers, G. S. Lukat-Rodgers, J. L. DuBois, *Dalton Trans.* **2013**, *42*, 3156–3169.
80. D. C. de Geus, E. A. J. Thomassen, P.-L. Hagedoorn, N. S. Pannu, E. van Duijn, J. P. Abrahams, *J. Mol. Biol.* **2009**, *387*, 192–206.
81. A. Ebihara, A. Okamoto, Y. Kousumi, H. Yamamoto, R. Masui, N. Ueyama, S. Yokoyama, S. Kuramitsu, *J. Struct. Funct. Gen.* 2005, *6*, 21–32.
82. J. Kostan, B. Sjoeblom, F. Maixner, G. Mlynek, P. G. Fürtmueller, C. Obinger, M. Wagner, H. Daims, K. Djinovic-Carugo, *J. Struct. Biol.* **2010**, *172*, 331–342.
83. B. Goblirsch, R. C. Kurker, B. R. Streit, C. M. Wilmot, J. L. DuBois, *J. Mol. Biol.* **2011**, *408*, 379–398.
84. E. P. Skaar, A. H. Gaspar, O. Schneewind, *J. Biol. Chem.* **2004**, *279*, 436–443.
85. R. Y. Wu, E. P. Skaar, R. G. Zhang, G. Joachimiak, P. Gornicki, O. Schneewind, A. Joachimiak, *J. Biol. Chem.* **2005**, *280*, 2840–2846.
86. W. C. Lee, M. L. Reniere, E. P. Skaar, M. E. Murphy, *J. Biol. Chem.* **2008**, *283*, 30957–30963.
87. Y. Sugano, R. Muramatsu, A. Ichiyanagi, T. Sato, M. Shoda, *J. Biol. Chem.* **2007**, *282*, 36652–36658.
88. M. Ahmad, J. N. Roberts, E. M. Hardiman, R. Singh, L. D. Eltis, T. D. H. Bugg, *Biochemistry* **2011**, *50*, 5096–5107.
89. J. A. Mayfield, B. Blanc, K. R. Rodgers, G. S. Lukat-Rodgers, J. L. DuBois, *Biochemistry* **2013**, *52*, 6982–6994.
90. S. Adachi, S. Nagano, K. Ishimori, Y. Watanabe, I. Morishima, T. Egawa, T. Kitagawa, R. Makino, *Biochemistry* **1993**, *32*, 241–252.
91. A. Farhana, V. Saini, A. Kumar, J. R. Lancaster, Jr., A. J. C. Steyn, *Antiox. Redox Signal.* 2012, *17*, 1232–1245.
92. G. S. Lukat-Rodgers, K. R. Rodgers, *J. Biol. Inorg. Chem.* 1998, *3*, 274–281.
93. W. Gong, B. Hao, M. K. Chan, *Biochemistry* **2000**, *39*, 3955–3962.
94. S. Aono, H. Nakajima, *Coord. Chem. Rev.* **1999**, *192*, 267–282.
95. T. L. Poulos, *Curr. Opin. Struct. Biol.* **2006**, *16*, 736–743.
96. K. Choudhury, M. Sundaramoorthy, A. Hickman, T. Yonetani, E. Woehl, M. F. Dunn, T. L. Poulos, *J. Biol. Chem.* **1994**, *269*, 20239–20249.
97. T. L. Poulos, R. E. Fenna, in *Metal Ions in Biological Systems,* Vol. 30, Eds H. Sigel, A. Sigel, Marcel Dekker, Inc., New York, 1994, pp. 25–75.
98. B. R. Streit, B. Blanc, G. S. Lukat-Rodgers, K. R. Rodgers, J. L. DuBois, *J. Am. Chem. Soc.* **2010**, *132*, 5711–5724.
99. D. M. Davies, P. Jones, D. Mantle, *Biochem. J.* **1976**, *157*, 247–253.
100. P. Jones, H. B. Dunford, *J. Theor. Biol.* **1977**, *69*, 457–470.
101. J. E. Erman, L. B. Vitello, M. A. Miller, J. Kraut, *J. Am. Chem. Soc.* **1992**, *114*, 6592–6593.
102. S. Hofbauer, M. Bellei, A. Suendermann, K. F. Pirker, A. Hagmueller, G. Mlynek, J. Kostan, H. Daims, P. G. Fürtmueller, K. Djinovic-Carugo, C. Oostenbrink, G. Battistuzzi, C. Obinger, *Biochemistry* **2012**, *51*, 9501–9512.
103. S. Hofbauer, K. Gysel, G. Mlynek, J. Kostan, A. Hagmueller, H. Daims, P. G. Furtmueller, K. Djinovic-Carugo, C. Obinger, *Biochim. Biophys. Acta* **2012**, *1824*, 1031–1038.
104. DuBois lab, unpublished results.
105. B. R. Streit, J. L. DuBois, *Biochemistry* **2008**, *47*, 5271–5280.
106. A. Q. Lee, B. R. Streit, M. Zdilla, M. A. Abu-Omar, J. L. DuBois, *Proc. Natl. Acad. Sci. USA* **2008**, *105*, 15654–15659.
107. Y. Patel, D. Wong, L. Ingerman, P. McGinnis, M. Osier, Environmental Protection Agency report: "Toxicological Review of Chlorine Dioxide and Chlorite", **2000**; available for download from the world wide web.
108. R. A. Miller, B. E. Britigan, *Clin. Microbiol. Rev.* **1997**, *10*, 1–18.

109. U. K. Klaning, K. Sehested, J. Holcman, *J. Phys. Chem.* **1985**, *89*, 760–763.
110. H. B. Dunford, *Heme Peroxidases*, Wiley-VCH, New York, USA, 1999, pp. 528.
111. A. Gumiero, C. L. Metcalfe, A. R. Pearson, E. L. Raven, P. C. Moody, *J. Biol. Chem.* **2011**, *286*, 1260–1268.
112. T. A. Betley, Q. Wu, T. Van Voorhis, D. G. Nocera, *Inorg. Chem.* **2008**, *47*, 1849–1861.
113. I. Rivalta, G. W. Brudvig, V. S. Batista, *Curr. Opin. Chem. Biol.* **2012**, *16*, 11–18.
114. J. B. Lee, J. A. Hunt, J. T. Groves, *J. Am. Chem. Soc.* **1998**, *120*, 7493–7501.
115. J. Groves, J. Lee, J. Hunt, R. Shimanovich, N. Jin, *J. Inorg. Biochem.* **1999**, *74*, 28–28.
116. J. Su, J. Groves, *J. Am. Chem. Soc.* **2009**, *131*, 12979–12988.
117. J. Su, J. Groves, *Inorg. Chem.* **2010**, *49*, 6317–6329.
118. L. M. K. Dassama, T. H. Yosca, D. A. Conner, M. H. Lee, B. Blanc, B. R. Streit, M. T. Green, J. L. DuBois, C. Krebs, J. M. Bollinger, Jr., *Biochemistry* **2012**, *51*, 1607–1616.
119. J. L. DuBois, J. M. Mayfield, "Dioxygen-Generating Chlorite Dismutases and the CDE Protein Superfamily", Chapter 90 in *Handbook of Porphyrin Science*, Vol. 19, Eds K. M. Kadish, K. M. Smith, and R. Guilard, World Scientific, Singapore, 2012, pages 231–283.
120. C. Jakopitsch, H. Spalteholz, P. G. Fürtmuller, J. Arnhold, C. Obinger, *J. Inorg. Biochem.* **2008**, *102*, 293–302.
121. A. Gumiero, E. J. Murphy, C. L. Metcalfe, P. C. E. Moody, E. L. Raven, *Arch. Biochem. Biophys.* **2010**, *500*, 13–20.
122. A. N. Hiner, E. L. Raven, R. N. Thorneley, F. García-Cánovas, J. N. Rodríguez-López, *J Inorg. Biochem.* **2002**, *91*, 27–34.
123. J. E. Erman, L. B. Vitello, M. A. Miller, A. Shaw, K. A. Brown, J. Kraut, *Biochemistry* **1993**, *32*, 9798–9806.
124. B. C. Finzel, T. L. Poulos, J. Kraut, *J. Biol. Chem.* **1984**, *259*, 3027–3036.
125. S. L. Edwards, N. H. Xuong, R. C. Hamlin, J. Kraut, *Biochemistry* **1987**, *26*, 1503–1511.
126. J. Hernandez-Ruiz, M. B. Arnao, A. N. P. Hiner, F. Garcia-Canovas, M. Acosta, *Biochem. J.* **2001**, *354*, 107–114.
127. A. N. P. Hiner, J. N. Rodriguez-Lopez, M. B. Arnao, E. L. Raven, F. Garcia-Canovas, M. Acosta, *Biochem. J.* **2000**, *348*, 321–328.
128. J. N. Rodriguez-Lopez, J. Hernandez-Ruiz, F. Garcia-Canovas, R. N. F. Thorneley, M. Acosta, M. B. Arnao, *J. Biol. Chem.* **1997**, *272*, 5469–5476.
129. S. L. Edwards, T. L. Poulos, *J. Biol. Chem.* **1990**, *265*, 2588–2595.
130. J. A. Gustafsson, E. G. Hrycay, L. Ernster, *Arch. Biochem. Biophys.* **1976**, *174*, 440–453.
131. J. M. Pratt, T. I. Ridd, L. J. King, *J. Chem. Soc., Chem. Commun.* **1995**, *22*, 2297–2298.
132. L. M. Slaughter, J. P. Collman, T. A. Eberspacher, J. I. Brauman, *Inorg. Chem.* **2004**, *43*, 5198–5204.
133. J. P. Collman, H. Tanaka, R. T. Hembre, J. I. Brauman, *J. Am. Chem. Soc.* **1990**, *112*, 3689–3690.
134. M. M. Abu-Omar, *Dalton Trans.* **2011**, *40*, 3435–3444.
135. M. J. Zdilla, A. Q. Lee, M. M. Abu-Omar, *Angew. Chem. Int. Ed. Engl.* **2008**, *47*, 7697–7700.
136. M. J. Zdilla, A. Q. Lee, M. M. Abu-Omar, *Inorg. Chem.* **2009**, *48*, 2260–2268.
137. T. P. Umile, J. T. Groves, *Angew. Chem. Int. Ed. Engl.* **2011**, *50*, 695–698.
138. S. D. Hicks, J. L. Petersen, C. J. Bougher, M. M. Abu-Omar, *Angew. Chem. Int. Ed. Engl.* **2011**, *50*, 699–702.
139. W. D. Hewson, L. P. Hager, *J. Biol. Chem.* **1979**, *254*, 3175–3181.
140. S. Shahangian, L. P. Hager, *J. Biol. Chem.* **1982**, *257*, 1529–1533.
141. H. B. Dunford, R. A. Alberty, *Biochemistry* **1967**, *6*, 447.
142. M. A. Ator, S. K. David, P. R. O. De Montellano, *J. Biol. Chem.* **1987**, *262*, 14954–14960.
143. M. A. Ator, P. R. O. Demontellano, *J. Biol. Chem.* **1987**, *262*, 1542–1551.
144. P. R. O. Demontellano, S. K. David, M. A. Ator, D. Tew, *Biochemistry* **1988**, *27*, 5470–5476.
145. A. Wolterink, S. Kim, M. Muusse, I. S. Kim, P. J. M. Roholl, C. G. van Ginkel, A. J. M. Stams, S. W. M. Kengen, *Int. J. System. Evol. Microbiol.* **2005**, *55*, 2063–2068.
146. B. C. Okeke, W. T. Frankenberger, *Microbiol. Res.* **2003**, *158*, 337–344.

147. L. M. Steinberg, J. J. Trimble, B. E. Logan, *FEMS Microbiol. Lett.* **2005**, *247*, 153–159.
148. A. Wolterink, E. Schiltz, P. Hagedoorn, W. Hagen, S. Kengen, A. Stams, *J. Bacteriol.* **2003**, *185*, 3210–3213.
149. H. D. Thorell, N. H. H. Beyer, N. H. H. Heegaard, M. Ohman, T. Nilsson, *Eur. J. Biochem.* **2004**, *271*, 3539–3546.
150. K. Stenklo, H. D. Thorell, H. Bergius, R. Aasa, T. Nilsson, *J. Biol. Inorg. Chem.* **2001**, *6*, 601–607.
151. S. W. M. Kengen, G. B. Rikken, W. R. Hagen, C. G. van Ginkel, A. J. M. Stams, *J. Bact.* **1999**, *181*, 6706–6711.
152. F. Mehboob, A. F. M. Wolterink, A. J. Vermeulen, B. Jiang, P.-L. Hagedoorn, A. J. M. Stams, S. W. M. Kengen, *FEMS Microbiol. Lett.* **2009**, *293*, 115–121.
153. Å. Malmqvist, T. Welander, E. Moore, A. Ternström, G. Molin, I. Stenström, *Syst. Appl. Microbiol.* **1994**, *17*, 58–64.
154. H. Danielsson Thorell, K. Stenklo, J. Karlsson, T. Nilsson, *Appl. Environ. Microbiol.* **2003**, *69*, 5585–5592.
155. J. L. DuBois, C. J. Carrell, C. M. Wilmot, "Reactivity and Structure in the CDE Protein Superfamily: from O_2 Generation to Peroxidase Chemistry and Beyond", in *Handbook of Porphyrin Science*, Vol. 26, Ed G. Ferreira, World Scientific, Singapore, 2013, pp. 442–470.